

# Stellar Astrophysics

Summer of Science - Endterm Report

Vaishnav V. Rao  
Roll no. 190260045  
Mentor- Himansh Rathore

# Contents

0.1	Introduction . . . . .	iii
<b>1</b>	<b>Prerequisites</b>	<b>1</b>
1.1	The method of trigonometric parallax . . . . .	1
1.2	The Magnitude Scale and more . . . . .	1
1.3	The Theory of Special Relativity . . . . .	2
1.3.1	Time Dilation & Length Contraction . . . . .	3
1.3.2	Relativistic Doppler Effect . . . . .	3
1.3.3	Relativistic Momentum and Energy . . . . .	4
<b>2</b>	<b>Binary Systems and Stellar Parameters</b>	<b>5</b>
2.1	Mass determination using visual binaries . . . . .	5
2.2	Eclipsing Spectroscopic Binaries . . . . .	6
2.2.1	Variation of velocity . . . . .	6
2.2.2	Mass Function . . . . .	6
2.2.3	Using eclipses to find radii and ratio of temperatures . . . . .	7
<b>3</b>	<b>Classification of Stellar Spectra</b>	<b>9</b>
3.1	The Harvard Classification of Stellar Spectra . . . . .	9
3.2	Some Statistical Physics . . . . .	9
3.3	H-R Diagrams . . . . .	11
<b>4</b>	<b>Stellar Atmospheres</b>	<b>13</b>
4.1	The Radiation Field . . . . .	13
4.1.1	Specific and Mean Intensities . . . . .	13
4.1.2	Specific Energy density, Radiative Flux and Radiation Pressure . . . . .	14
4.2	Stellar Opacity . . . . .	14
4.2.1	Definition of opacity . . . . .	14
4.2.2	Optical depth . . . . .	15
4.3	Transfer equation and Radiation Pressure gradient . . . . .	16
4.4	Eddington Approximation . . . . .	16
4.5	Limb Darkening . . . . .	17
<b>5</b>	<b>The Sun</b>	<b>18</b>
5.1	The Solar Neutrino Problem . . . . .	18
5.2	The Parker Solar Wind Model . . . . .	19
5.3	Hydrodynamic nature of the upper solar atmosphere . . . . .	19
5.4	Magnetohydrodynamics (MHD) and Alfvén waves . . . . .	20
5.5	The Solar Cycle . . . . .	21
5.5.1	Sunspots . . . . .	21

5.5.2	The Magnetic Dynamo Model . . . . .	22
<b>6</b>	<b>Interior of Stars</b>	<b>23</b>
6.1	Hydrostatic Equilibrium and Mass conservation . . . . .	23
6.2	Pressure Equation of State . . . . .	23
6.3	Stellar Energy Sources . . . . .	25
6.3.1	Timescales . . . . .	25
6.3.2	Quantum Tunneling . . . . .	25
6.3.3	Nuclear Reaction Rates and the Gamow Peak . . . . .	27
6.3.4	Luminosity Gradient . . . . .	27
6.3.5	Stellar Nuclear reactions . . . . .	28
6.4	Energy Transport and Thermodynamics . . . . .	29
6.4.1	The radiative temperature gradient . . . . .	29
6.4.2	The adiabatic temperature gradient . . . . .	30
6.4.3	Mixing Length Theory of superadiabatic convection . . . . .	30
6.5	Stellar Model Building . . . . .	31
6.5.1	Constitutive relations and Boundary Conditions . . . . .	32
6.5.2	Lane-Emden Equations and Polytropic Models . . . . .	32
6.6	Main Sequence and Eddington Luminosity limit . . . . .	33
<b>7</b>	<b>Star Formation</b>	<b>34</b>
7.1	Formation of protostars . . . . .	34
7.1.1	Jeans Criterion . . . . .	34
7.1.2	Homologous Collapse . . . . .	35
7.1.3	Fragmentation of Collapsing Clouds . . . . .	36
7.1.4	Additional processes in protostar formation . . . . .	37
7.2	Evolutionary Tracks . . . . .	37
7.3	Pre-main sequence evolution . . . . .	38
<b>8</b>	<b>Main Sequence and Post Main Sequence evolution</b>	<b>40</b>
8.1	Low-mass main-sequence evolution . . . . .	40
8.2	Schönberg-Chandrasekhar limit . . . . .	41
8.3	Post Main Sequence Evolution . . . . .	42
8.4	Helium core flash . . . . .	43
<b>9</b>	<b>Stellar Pulsation</b>	<b>44</b>
9.1	Period Luminosity relation . . . . .	44
9.2	Physics of Stellar Pulsation . . . . .	45
9.2.1	Period-Density Relation . . . . .	45
9.2.2	The Eddington valve mechanism . . . . .	45
9.3	Modeling Stellar Pulsation . . . . .	46
9.4	Non-radial Stellar Pulsation . . . . .	47
9.4.1	p-modes . . . . .	47
9.4.2	g-modes and the buoyancy frequency . . . . .	48
<b>10</b>	<b>Degenerate Remnants of Stars</b>	<b>49</b>
10.1	White Dwarfs . . . . .	49
10.1.1	Physics of Degenerate Matter . . . . .	49

10.1.2 Electron Degeneracy Pressure . . . . .	50
10.1.3 Chandrashekhar Limit . . . . .	51
10.1.4 Cooling of White Dwarfs . . . . .	51
10.2 Neutron Stars . . . . .	53
10.2.1 Formation and Properties . . . . .	53
10.2.2 Rapid Rotation and Conservation of Angular Momentum . . . . .	54
10.2.3 Magnetic Fields . . . . .	54

## 0.1 Introduction

Stellar astrophysics is a subject that deals with understanding the structure, dynamics and evolution of stars through the natural laws of physics with the help of observational astronomy. This subject is considered to be a resounding success of classical and modern physics as theoretical models are in excellent agreement with observed phenomena. This is a report of my study of the subject.

We start off with some prerequisites of special relativity and general astronomy and then dive into the physics of stellar structure. Proceeding through stellar evolution (touching a bit of stellar dynamics through stellar pulsation on the way), we conclude the study with the death of stars. So, join me on this 10 chapter journey as we unravel the mysteries of stars.

# Chapter 1

## Prerequisites

### 1.1 The method of trigonometric parallax

Reasonable estimates of the distances to celestial bodies in the Milky Way galaxy (our galaxy) and its local neighbourhood can be made with the method of trigonometric parallax. This method employs the measurement of the angular displacement of the object in question when measured from two points separated by a finite distance. After this, finding the distance to the object is a matter of simple trigonometry provided the finite displacement between the points of measurement is known (Fig 1.1).

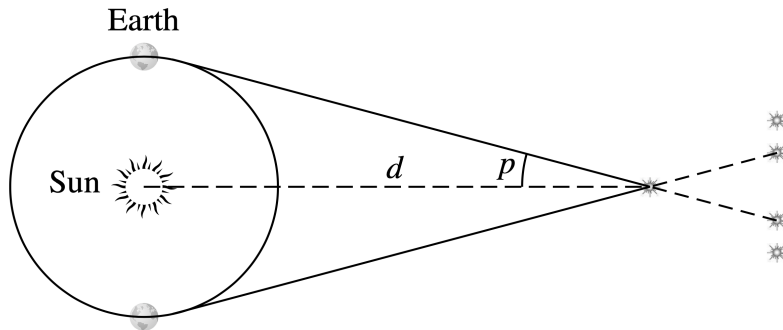


Figure 1.1: Measurement of parallax angle  $p$  [1].

As the distance from the Earth to the Sun is 1 Astronomical Unit (AU),

$$d = \frac{1 \text{ AU}}{\tan p} \simeq \frac{1}{p} \text{ AU}$$

Here, the approximation  $\tan p \simeq p$  has been made for parallax angle  $p$  measured in *radians*. Alternatively, defining a parsec (parallax-second -pc) to be the distance at which an object subtends 1 *arcsecond*, we have,

$$d = \frac{1}{p''} \text{ pc}$$

### 1.2 The Magnitude Scale and more

The radiant flux  $F$  measured at a distance  $r$  from a star of luminosity  $L$  is

$$F = \frac{L}{4\pi r^2} \quad (1.1)$$

Here we define apparent magnitude  $m$  in such a way that a difference of 5 magnitudes between the apparent magnitudes of two stars corresponds to the smaller-magnitude star being 100 times brighter than the larger-magnitude star. Hence,

$$\frac{F_2}{F_1} = 100^{(m_1 - m_2)/5} \quad (1.2)$$

Absolute magnitude  $M$  is defined as the apparent magnitude of the star if it were at a distance of 10 pc from us. Hence, from Eq 1.1 and 1.2, we have

$$m - M = 5 \log_{10} \left( \frac{d}{10pc} \right) \quad (1.3)$$

where  $d$  is the distance to the star and  $m - M$  is called the distance modulus.

In accordance with Stefan's law, we define effective temperature  $T_e$  according to the equation

$$L = 4\pi R^2 \sigma T_e^4 \quad (1.4)$$

where  $L$  is the star's luminosity and  $R$  is the star's radius.

### 1.3 The Theory of Special Relativity

Einstein's theory of Special Relativity stems out of the inability of Galilean Relativity to explain the constancy of speed of light across all inertial frames of reference, in accordance with experiments. The theory itself is based on the following two postulates given by Einstein:

- The Principle of Relativity: The laws of physics are the same in all inertial reference frames.
- The Constancy of the Speed of Light: Light moves through a vacuum at a constant speed  $c$  that is independent of the motion of the light source.

A direct consequence of these postulates are the phenomena of length contraction and time dilation.

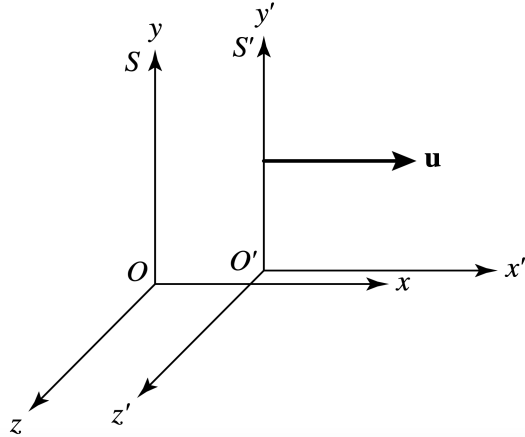


Figure 1.2: Inertial frames  $S$  and  $S'$ .

### 1.3.1 Time Dilation & Length Contraction

For two inertial frames of reference  $S$  and  $S'$  moving with respect to each other as shown above, it is possible to derive the following Lorentz transformation equations using the two postulates and symmetry arguments.

$$\begin{aligned}x' &= \frac{x - ut}{\sqrt{1 - u^2/c^2}} \\y' &= y \quad z' = z \\t' &= \frac{t - ux/c^2}{\sqrt{1 - u^2/c^2}}\end{aligned}\tag{1.5}$$

Here we define the Lorentz factor

$$\gamma = \frac{1}{\sqrt{1 - u^2/c^2}}$$

Suppose light is emitted at intervals of  $\Delta t_{rest}$  at a fixed location in  $S'$ , then according to Eq. set 1.5, the time interval  $\Delta t_{moving}$  between successive light emissions as measured from  $S$  is

$$\Delta t_{moving} = \gamma \Delta t_{rest}\tag{1.6}$$

In other words, the time measured from a frame in which the source appears to be moving is *dilated* with respect to the time measured in the frame in which the source is at rest.

Now, if we consider a rod of length  $L_{rest}$  to be at rest in frame  $S'$  and make measurements of the positions of the ends of the rod simultaneously from frame  $S$ , we get the length of the rod  $L_{moving}$  in frame  $S$  to be

$$L_{moving} = L_{rest}/\gamma\tag{1.7}$$

In other words, the length of the rod as measured from a frame in which the rod appears to be moving is *contracted* with respect to the length of the rod measured from the frame in which the rod is at rest.

### 1.3.2 Relativistic Doppler Effect

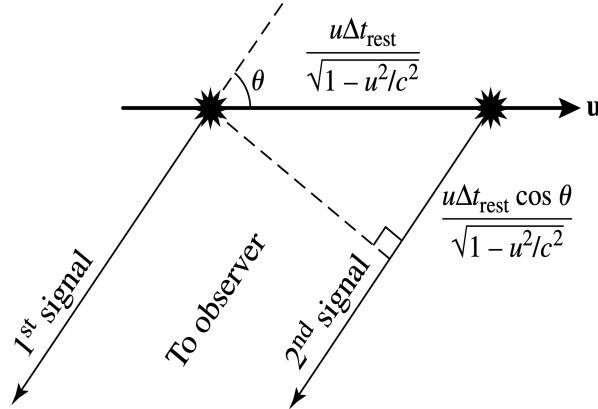


Figure 1.3: Relativistic Doppler Shift [1].

The above figure shows a source of light moving with a velocity  $u$  and emitting light at intervals of  $\Delta t_{rest}$  (frequency  $\nu_{rest} = 1/\Delta t_{rest}$ ) in the frame in which it is at rest. For the special case where  $\theta = 0^\circ$  or  $180^\circ$ , we get the observed frequency with which the source is emitting light  $\nu_{obs}$  as

$$\nu_{obs} = \nu_{rest} \sqrt{\frac{1 - v_r/c}{1 + v_r/c}} \implies \lambda_{obs} = \lambda_{rest} \sqrt{\frac{1 + v_r/c}{1 - v_r/c}} \quad (1.8)$$

where  $v_r$  is the relative speed with which the source is moving *away* from the observer. From the point of view of astronomy, we also define a redshift parameter

$$z = \frac{\lambda_{obs} - \lambda_{rest}}{\lambda_{rest}} = \frac{\Delta\lambda}{\lambda_{rest}} = \sqrt{\frac{1 + v_r/c}{1 - v_r/c}} - 1 = \frac{\Delta t_{obs}}{\Delta t_{rest}} - 1 \quad (1.9)$$

### 1.3.3 Relativistic Momentum and Energy

The relativistic momentum vector  $\vec{p}$  of a particle is defined as

$$\vec{p} = \gamma m \vec{v}$$

where  $\vec{v}$  is the particle's velocity with respect to the observer and  $m$  is the mass of the particle, *invariant* across all frames of reference. From this it is possible to derive the particle's kinetic energy  $K$  to be

$$K = mc^2(\gamma - 1)$$

Defining  $E$  to be the particle's total relativistic energy  $\gamma mc^2$  we get the following relation from the definition of momentum

$$E^2 = p^2 c^2 + m^2 c^4 \quad (1.10)$$

For the special case in which the particle is at rest, we get the famous relation

$$E = mc^2$$

Armed with these tools we will now dive into the realm of astrophysics.

## Chapter 2

# Binary Systems and Stellar Parameters

Studying astronomy is like reading a detective story. It involves making deductions about a star's size, mass, distance, composition, temperature, velocity, age and a thousand other things by just observing the light coming from it. In this section we see how we can determine the masses and temperatures of stars in binary systems just by making optical observations. But before we get into the detective work, let us see the different kinds of binary systems we shall come across in this section.

- Visual binary: Both stars in the binary can be resolved independently.
- Eclipsing binary: One star periodically passes in front of the other.
- Double-line Spectroscopic binary: Spectral lines of both stars are visible and the spectral lines alternately become single and double about a fixed wavelength  $\lambda_o$  due to the Doppler effect.

### 2.1 Mass determination using visual binaries

If the distance to a binary star system, whose orbital plane is perpendicular to our line of sight, is known (say using trigonometric parallax), the linear separation of the stars can be determined. From the basic force equations and conservation laws, the ratio of the masses of the stars is

$$\frac{m_1}{m_2} = \frac{r_2}{r_1} = \frac{a_2}{a_1} = \frac{\alpha_2}{\alpha_1} \quad (2.1)$$

where  $r_1$  and  $r_2$  are the distances of the stars from the centre of mass,  $a_1$  and  $a_2$  are the semi-major axes of the elliptical orbits and  $\alpha_1$  and  $\alpha_2$  are the angles subtended by the semi-major axes (as  $\alpha = a/d$ , where  $d$  is the distance to the binary system)

Kepler's law in general form tells us:

$$T^2 = \frac{4\pi^2 a^3}{G(m_1 + m_2)} \quad (2.2)$$

where  $a = a_1 + a_2$ . Thus if  $a$  can be determined, the individual masses of the stars can be determined using Eq. 2.1. Further, if the plane of the ellipses is inclined at an angle  $i$  to the plane of the sky, we have

$$\begin{aligned} m_1 + m_2 &= \frac{4\pi^2 (\alpha d)^3}{GT^2} = \frac{4\pi^2}{G} \left( \frac{d}{\cos i} \right)^3 \tilde{\alpha}^3 \\ \frac{m_1}{m_2} &= \frac{\alpha_2}{\alpha_1} = \frac{\tilde{\alpha}_2 \cos i}{\tilde{\alpha}_1 \cos i} = \frac{\tilde{\alpha}_2}{\tilde{\alpha}_1} \end{aligned} \quad (2.3)$$

where  $\tilde{\alpha} = \tilde{\alpha}_1 + \tilde{\alpha}_2$ , the observed angles subtended by the semi-major axes.

## 2.2 Eclipsing Spectroscopic Binaries

### 2.2.1 Variation of velocity

For double-line spectroscopic binary systems, the radial velocities of the two stars can be determined through Doppler shifts. If we assume the orbits to be circular and the orbital plane to be in the line of sight ( $i = 90^\circ$ ), the measured radial velocities of the two stars will be sinusoidal. For the cases  $i \neq 90^\circ$ , the maximum measured radial velocities will be scaled by a factor of  $\sin i$  and the radial velocities themselves will remain sinusoidal but lesser in amplitude. If the orbits are elliptical, the observed radial velocity curves become skewed and non-sinusoidal.

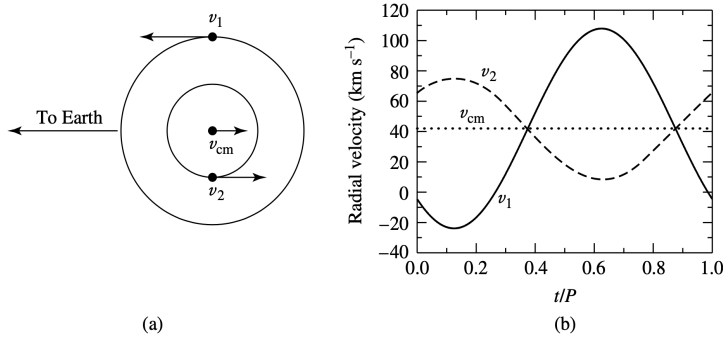


Figure 2.1: The orbital paths and radial velocities of two stars in circular orbits. (a) The plane of the orbits lie along the line of sight of observer. (b) The observed radial velocity curves [1].

### 2.2.2 Mass Function

If the eccentricity of the elliptical orbits  $e \ll 1$ , the orbital speeds are almost constant. Hence,  $v_1 = 2\pi a_1/T$  and  $v_2 = 2\pi a_2/T$ . Thus from Eq. 2.1, we have

$$\frac{m_1}{m_2} = \frac{v_2}{v_1} = \frac{v_{2r}/\sin i}{v_{1r}/\sin i} = \frac{v_{2r}}{v_{1r}} \quad (2.4)$$

where  $v_{1r}$  and  $v_{2r}$  are the observed radial velocities. Now,  $a = a_1 + a_2 = T/2\pi(v_1 + v_2)$ . Using this in Eq. 2.2,

$$m_1 + m_2 = \frac{T(v_{1r} + v_{2r})^3}{2\pi G \sin^3 i}$$

For single line spectroscopic binaries, say star 1 is observable and star 2 is not. This means only  $v_{1r}$  is measurable. Using the above two equations we arrive at

$$\frac{m_2^3}{(m_1 + m_2)^2} \sin^3 i = \frac{T}{2\pi G} v_{1r}^3 \quad (2.5)$$

The term on the RHS is called mass function as it is a function of readily observable quantities. If either  $m_1$  or  $i$  is unknown, the mass function sets a lower limit for  $m_2$  as the LHS is always lesser than  $m_2$ .

### 2.2.3 Using eclipses to find radii and ratio of temperatures

If a binary star system is observed to be an eclipsing binary, it is reasonable to take  $i \approx 90^\circ$ . Further the radii of these stars can be determined by using the duration of these eclipses and the radial velocities of the stars. The following figure illustrates this

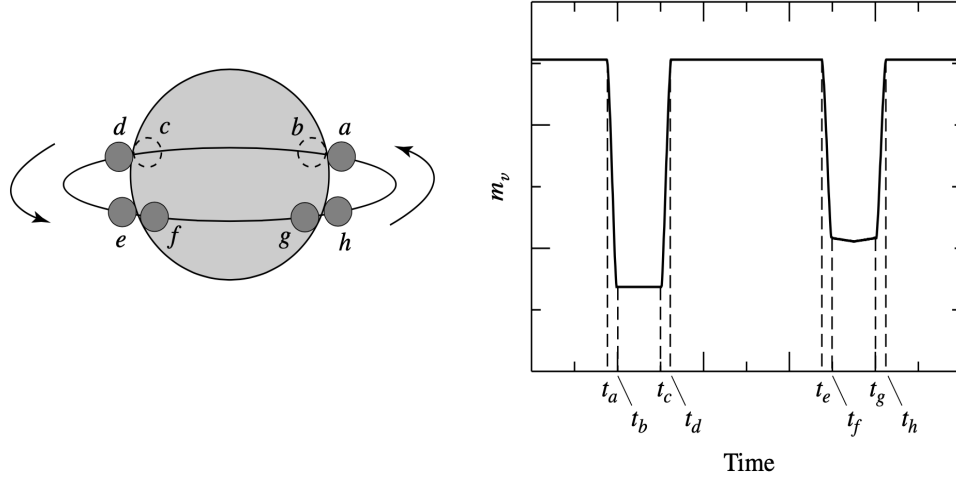


Figure 2.2: The light curve for an eclipsing binary with  $i \approx 90^\circ$ . The times indicated on the light curve correspond to the positions of the smaller star relative to its larger companion. It is assumed that the smaller star is hotter [1].

Assuming  $a_s \gg r_s, r_l$  (the radii of the smaller and larger star), we have

$$\begin{aligned} r_s &= v/2(t_b - t_a) \\ r_l &= v/2(t_c - t_a) \end{aligned} \quad (2.6)$$

where  $v = v_s + v_l$  is the relative velocity of one star with respect to the other (orbital speeds are typically non relativistic).

The ratio of temperatures of eclipsing binaries can also be determined from the light curves. We know that the radiative surface flux is given by  $F_r = \sigma T_e^4$  from Eq. 1.1. Thus the amount of light detected when both the stars are visible is given by

$$B_0 = k(\pi r_l^2 F_{rl} + \pi r_s^2 F_{rs}) \quad (2.7)$$

where  $k$  is a constant that is dependent on the distance to the system and the nature of the detector.

Similarly, the amount of light detected during the primary minima of the light curve (when the smaller star is behind) and the secondary minima (when the smaller star is in front) is

$$\begin{aligned} B_p &= k\pi r_l^2 F_{rl} \\ B_s &= k(\pi r_l^2 - \pi r_s^2)F_{rl} + k\pi r_s^2 F_{rs} \end{aligned} \quad (2.8)$$

Since it is not possible to determine  $k$ , ratios are employed.

$$\frac{B_0 - B_p}{B_0 - B_s} = \frac{F_{rs}}{F_{rl}} = \left( \frac{T_s}{T_l} \right)^4 \quad (2.9)$$

A notable thing to mention at this point is that extraterrestrial planets have been discovered by observing the dimming of starlight caused by the transit of planets in front of their parent stars. Another method of detecting extraterrestrial planets is measuring the radial velocity variations of the parent star induced by the *gravitational tug* of the planet. To get an idea of just how unbelievably small these variations can be, the radial velocity variation of the Sun due to Jupiter is roughly 12 m/s. Similar to the speed of a world class sprinter from Earth!

# Chapter 3

## Classification of Stellar Spectra

### 3.1 The Harvard Classification of Stellar Spectra

<b>Spectral Type</b>	<b>Temperature (Kelvin)</b>	<b>Spectral Lines</b>
O	28,000 - 50,000	Ionized helium
B	10,000 - 28,000	Helium, some hydrogen
A	7500 - 10,000	Strong hydrogen, some ionized metals
F	6000 - 7500	Hydrogen, ionized calcium (labeled H and K on spectra) and iron
G	5000 - 6000	Neutral and ionized metals, especially calcium; strong G band
K	3500 - 5000	Neutral metals, sodium
M	2500 - 3500	Strong titanium oxide, very strong sodium

Figure 3.1: The table above shows some characteristic emission and absorption lines of each type of star [2].

### 3.2 Some Statistical Physics

Stellar classification is based on the fact that different spectral lines have different strengths at different temperatures. We now aim to explain this phenomenon through statistical physics. In this section we take the case of the Balmer absorption line.

We know that the no. of gas particles per unit volume having speeds between  $v$  and  $v + dv$  is given by the Maxwell-Boltzmann Distribution.

$$n_v dv = n \left( \frac{m}{2\pi kT} \right)^{3/2} e^{-mv^2/2kT} 4\pi v^2 dv \quad (3.1)$$

where  $n$  = total no. density and  $n_v = \partial n / \partial v$ .

The atoms of a gas gain and lose energy through collisions. As a result, the distribution in the speeds of impacting atoms produces a definite distribution of electrons among the atomic orbitals. Let  $s_a$  be a specific set of quantum no.s that identifies a state of energy  $E_a$  for a system of particles. The ratio of the probability  $P(s_b)$  that the system is in state  $s_b$  to the probability  $P(s_a)$  that the system is in state  $s_a$  is given by the Boltzmann equation.

$$\frac{P(s_b)}{P(s_a)} = \frac{e^{-E_b/kT}}{e^{-E_a/kT}} = e^{-(E_b-E_a)/kT} \quad (3.2)$$

Now, we define  $g_a$  and  $g_b$  to be the no. of states with energies  $E_a$  and  $E_b$  respectively (statistical weights). Then, the ratio of probabilities of finding an atom having energies  $E_b$  and  $E_a$  in the system is

$$\frac{P(E_b)}{P(E_a)} = \frac{g_b e^{-E_b/kT}}{g_a e^{-E_a/kT}} = \frac{g_b}{g_a} e^{-(E_b-E_a)/kT} = \frac{N_b}{N_a} \quad (3.3)$$

which is also the ratio of no. of atoms  $N_b$  and  $N_a$  (in different states of excitation) having energies  $E_b$  and  $E_a$ .

Applying only the Boltzmann equation to a gas of neutral hydrogen atoms where equal no. of atoms occupy the ground and first excited states, we get a temperature of around 85,000 K. This means that for a significant no. of atoms to occupy the first excited state, very high temperatures are required. But, as observations reveal, Balmer absorption line intensities peak at much lower temperatures of around 9,500 K. The answer to this discrepancy lies in considering the relative no. of atoms in different stages of *ionization*. The Saha equation gives us this relative no.

We define a partition function

$$Z_i = \sum_{j=1}^{\infty} g_j e^{-(E_j-E_i)/kT}$$

For all further considerations,  $i = 1$  is taken to be the non-ionised stage.

Now, the ratio of no. of atoms in ionisation stage  $i + 1$  to no. of atoms in ionisation stage  $i$  is

$$\frac{N_{i+1}}{N_i} = \frac{2Z_{i+1}}{n_e Z_i} \left( \frac{2\pi m_e k T}{h^2} \right)^{3/2} e^{-\chi_i/kT} \quad (3.4)$$

where  $\chi_i$  is the ionization energy needed to remove an electron from an atom or ion (in the ground state) thus taking it from ionisation stage  $i$  to ionisation stage  $i + 1$ .  $n_e$  is the free electron no. density.

Before combining the Saha and Boltzmann equations, we familiarise ourselves with the following terms:

$N_I$ : no. of non-ionised hydrogen atoms

$N_1$ : no. of hydrogen atoms in ground state

$N_{II}$ : no. of singly ionised hydrogen atoms

$N_2$ : no. of hydrogen atoms in 1<sup>st</sup> excited state

The strength of the Balmer absorption line depends on the ratio  $N_2/N_{total}$  i.e the fraction of *all* hydrogen atoms in the first excited state. At this point we make the reasonable approximation  $N_1 + N_2 \simeq N_I$  and write

$$\frac{N_2}{N_{total}} = \left( \frac{N_2}{N_1 + N_2} \right) \left( \frac{N_I}{N_{total}} \right) = \left( \frac{N_2/N_1}{1 + N_2/N_1} \right) \left( \frac{1}{1 + N_{II}/N_I} \right) \quad (3.5)$$

The individual ratios in the above equation can be found out using the Saha and Boltzmann equations. This equation can be thought of as the probability of finding the atom unionised *and* in the first excited state.

Now, if we plot  $N_2/N_{total}$  as a function of temperature after substituting the necessary values for the partition function, ionisation energy, and free electron density in a typical star, we get a maxima at approximately 9900 K in good agreement with observations.

### 3.3 H-R Diagrams

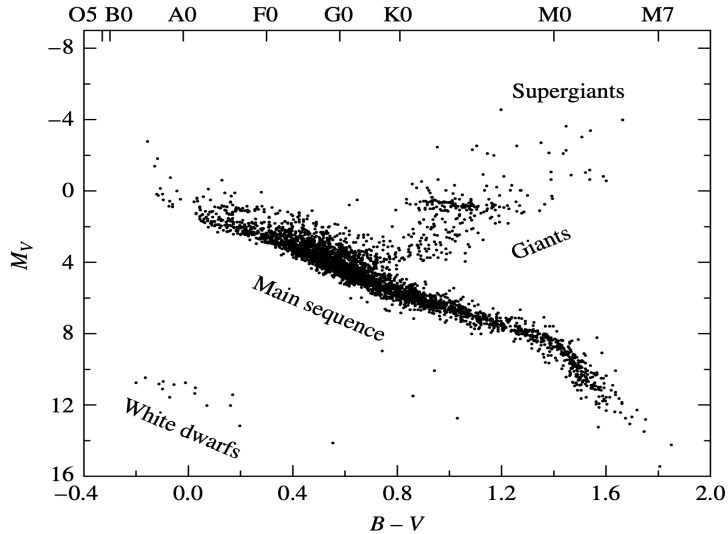


Figure 3.2: An observer's HR Diagram with data from the Hipparcos catalog [1].

A HR Diagram is a scatter plot of a star's absolute magnitude/luminosity vs. temperature/spectral class. In the above HR diagram, luminosity increases on moving up (as a lower magnitude implies higher luminosity) and temperature decreases on moving to the right. If two stars are of the same spectral type (approximately same effective temperature), a higher luminosity implies that the star is larger (from Eq 1.4). Thus, the groups in the HR Diagram have been labelled accordingly. With such a simple relation between temperature and luminosity, the position of the star on the main sequence is totally determined by the *mass* of the star, with mass increasing as we move up the main sequence.

Another question that arises is whether there is a difference in the spectra of giant and main sequence stars of the same spectral type. The answer is yes! It is found that for stars of the same spectral type, narrower spectral lines are produced by more luminous stars. This is the basis for the Morgan-Keenan luminosity classes.

Class	Type of Star
Ia-O	Extreme, luminous supergiants
Ia	Luminous supergiants
Ib	Less luminous supergiants
II	Bright giants
III	Normal giants
IV	Subgiants
V	Main-sequence (dwarf) stars
VI, sd	Subdwarfs
D	White dwarfs

Figure 3.3: The Morgan-Keenan luminosity classes [1].

These roman numerals are appended to the Harvard stellar classification of a star. Using both the types of stellar classification, the exact position of a star on the HR Diagram can now be determined by just reading the spectra of the star. The diagram itself is an important tool for finding the distances to stars by the method of main-sequence matching.

# Chapter 4

## Stellar Atmospheres

The light that astronomers receive from a star comes from the star's atmosphere, the layers of gas overlying the opaque interior. The temperature, density, and composition of the atmospheric layers from which these photons escape determine the features of the star's spectrum. To interpret the observed spectral lines properly, we must describe how light travels through the gas that makes up a star.

### 4.1 The Radiation Field

#### 4.1.1 Specific and Mean Intensities

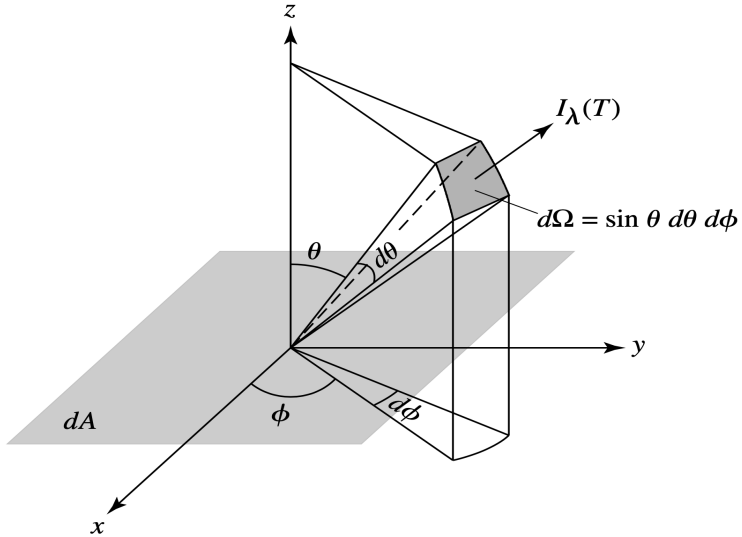


Figure 4.1: Intensity  $I_\lambda$  [1].

$E_\lambda d\lambda$  is assumed to be the amount of energy that rays with wavelengths in between  $\lambda$  and  $\lambda + d\lambda$ , emerging from a surface  $dA$ , carry into the cone in a time  $dt$  as shown in figure 5.3. Here,  $E_\lambda = \partial E / \partial \lambda$ . With this, the specific intensity of the rays is defined as

$$I_\lambda = \frac{\partial I}{\partial \lambda} = \frac{E_\lambda d\lambda}{d\lambda dt dA \cos \theta d\Omega} \quad (4.1)$$

Here,  $I_\lambda$  is defined in the limit  $d\Omega \rightarrow 0$ . Which means  $I_\lambda$  does not spread out and intensity of such a ray remains constant as it travels through empty space.

The mean intensity is the specific intensity averaged over all directions.

$$\langle I_\lambda \rangle = \frac{1}{4\pi} \int I_\lambda d\lambda = \frac{1}{4\pi} \int_{\phi=0}^{2\pi} \int_{\theta=0}^{\pi} I_\lambda \sin \theta d\theta d\phi \quad (4.2)$$

For an isotropic radiation field like black body radiation  $\langle I_\lambda \rangle = B_\lambda$  (the Planck Function).

#### 4.1.2 Specific Energy density, Radiative Flux and Radiation Pressure

The energy per unit volume in a radiation field having a wavelength between  $\lambda$  and  $\lambda + d\lambda$  is

$$u_\lambda d\lambda = \frac{4\pi}{c} \langle I_\lambda \rangle d\lambda \quad (4.3)$$

Specific radiative flux is the net energy having a wavelength between  $\lambda$  and  $\lambda + d\lambda$  that passes each second through a unit area int  $z$ -direction.

$$F_\lambda d\lambda = \int I_\lambda d\lambda \cos \theta d\Omega = \int_{\phi=0}^{2\pi} \int_{\theta=0}^{\pi} I_\lambda d\lambda \cos \theta \sin \theta d\theta d\phi \quad (4.4)$$

For an isotropic radiation field,  $F_\lambda = 0$  as there is no net transport of energy.

For a resolved source, what we measure as intensity, is the specific intensity, but for an unresolved source, what is being measured is the specific radiative flux.

It can also be derived that the specific radiation pressure of a photon 'gas' is given by

$$P_{rad,\lambda} = \frac{1}{c} \int_{sphere} I_\lambda d\lambda \cos^2 \theta d\Omega = \frac{4\pi}{3c} I_\lambda d\lambda \text{ for isotropic radiation} \quad (4.5)$$

## 4.2 Stellar Opacity

### 4.2.1 Definition of opacity

The change in intensity  $dI_\lambda$  of a light ray of wavelength  $\lambda$  as it passes through a gas, on account of absorption and scattering, is proportional to the intensity of the light ray, density of the gas and the distance  $ds$  travelled through it. Thus,

$$dI_\lambda = -\kappa_\lambda \rho I_\lambda ds \quad (4.6)$$

where  $\kappa_\lambda$  is the wavelength dependent absorption coefficient or opacity. The above equation can be integrated from some fixed reference point to get

$$I_\lambda = I_{\lambda,0} e^{-\int_0^s \kappa_\lambda \rho ds} \quad (4.7)$$

The characteristic distance travelled by a photon before being removed from the beam is taken to be

$$l = \frac{1}{\kappa_\lambda \rho} \quad (4.8)$$

### 4.2.2 Optical depth

For scattered photons, the characteristic distance  $l$  is in fact the mean free path of the photons, an expression which can be derived from statistical physics.

$$l = \frac{1}{\kappa_\lambda \rho} = \frac{1}{n \sigma_\lambda} \quad (4.9)$$

We now define wavelength dependent optical depth  $\tau_\lambda$ , back along a light ray as follows:

$$d\tau_\lambda = -\kappa_\lambda \rho ds \quad (4.10)$$

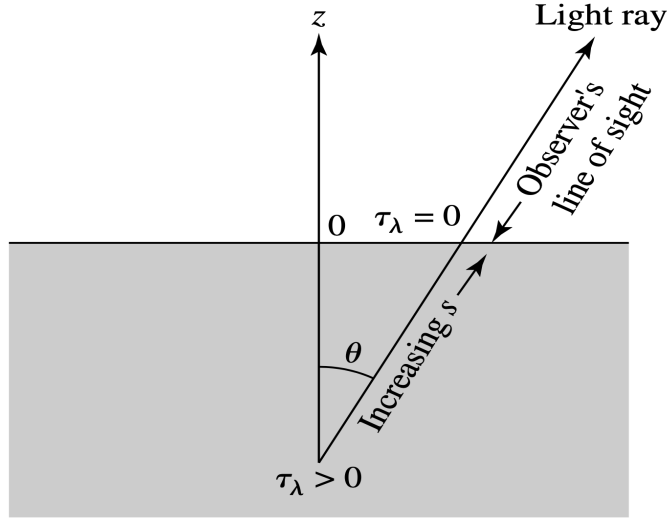


Figure 4.2: Optical depth  $\tau_{\lambda}$  measured back along a ray's path [1].

We can take the outermost layer of the star to be taken at optical depth  $\tau_\lambda = 0$  after which light travels unimpeded to the observer. The optical depth may be thought of as the no. of mean free paths from the original position to the surface as measured along the ray's path. As a result we typically see no deeper into an atmosphere at a given wavelength than  $\tau_\lambda \approx 1$ .

It is often useful to employ an opacity that has been averaged over all wavelengths so as to get an opacity that only depends on the composition, density and temperature. The most commonly used mean is the Rosseland Mean Opacity.

$$\frac{1}{\bar{\kappa}} = \frac{\int_0^\infty \frac{1}{\kappa_\nu} \frac{\partial B_\nu(T)}{\partial T} d\nu}{\int_0^\infty \frac{\partial B_\nu(T)}{\partial T} d\nu} \quad (4.11)$$

### 4.3 Transfer equation and Radiation Pressure gradient

If we consider absorption, emission *and* scattering, the change in intensity of a light ray as it travels a distance  $ds$  through the atmosphere is given by the transfer equation

$$\begin{aligned} dI_\lambda &= -\kappa_\lambda I_\lambda ds + j_\lambda \rho ds \\ \implies \frac{dI_\lambda}{d\tau_\lambda} &= I_\lambda - S_\lambda \end{aligned} \quad (4.12)$$

where  $S_\lambda = j_\lambda / \kappa_\lambda$  is called the source function.

If we make the assumption that the atmosphere is plane parallel, and gray (opacity does not depend on wavelength), replace  $I_\lambda$  and  $S_\lambda$  with  $I$  and  $S$  integrated over all wavelengths, and replace  $\tau$  with  $\tau_v$ , the vertical optical depth with the necessary scaling factor of  $1/\cos\theta$  as in figure 5.3, we get the following form of the transfer equation:

$$\cos\theta \frac{dI}{d\tau_v} = I - S \quad (4.13)$$

which can be integrated over all solid angles or multiplied by  $\cos\theta$  and integrated over all solid angles to get the following two equations from equations 4.4 and 4.5.

$$\begin{aligned} \frac{dF_{rad}}{d\tau_v} &= 4\pi(\langle I \rangle - \langle S \rangle) \\ \frac{dP_{rad}}{dr} &= -\frac{\bar{\kappa}\rho}{c} F_{rad} \end{aligned}$$

For equilibrium stellar atmospheres,  $F_{rad} = \text{const.} = F_{surf} = \sigma T_e^4$ . Thus the second equation can be integrated to get radiation pressure as a function of optical depth.

$$P_{rad} = \frac{1}{c} F_{rad} \tau_v + C \quad (4.14)$$

### 4.4 Eddington Approximation

If we knew how the radiation pressure varied with temperature for the general case we can use Eq. 4.14 to get a temperature profile of our plane-parallel, gray atmosphere. The Eddington approximation allows us to do just that. According to this, the intensity of radiation is assigned one value  $I_{out}$  in the  $+z$  direction and  $I_{in}$  in the  $-z$  direction. Here both  $I_{out}$  and  $I_{in}$  vary with depth and  $I_{in}$  is taken to be zero at the surface where  $\tau_v$  is zero. After working out the consequences of this approximation through the previous equations, it can be shown that

$$S = \langle I \rangle = \frac{3\sigma T_e^4}{4\pi} \left( \tau_v + \frac{2}{3} \right) \quad (4.15)$$

If we further assume that the atmosphere is in Local Thermodynamic Equilibrium, we get

$$T^4 = \frac{3}{4} T_e^4 \left( \tau_v + \frac{2}{3} \right) \quad (4.16)$$

which is the required temperature profile.

This equation tells us that the “surface” of a star, which by definition has temperature  $T_e$ , is not at the top of the atmosphere, where  $\tau_v = 0$ , but deeper down, where  $\tau_v = 2/3$ . This result may be thought of as the average point of origin of the observed photons. Thus, when looking at a star, we see down to a vertical optical depth of  $\tau_v \approx 2/3$ , averaged over the disk of the star.

## 4.5 Limb Darkening

It is observed that the *limbs* of stars are darker and less luminous compared to the centre of the star. We now aim to explain this phenomenon.

The second form of the transfer equation from equation group 4.12, can be multiplied with  $e^{-\tau_\lambda}$  and integrated from origin of the ray to top of the atmosphere to get emergent intensity  $I_\lambda(0)$  as

$$I_\lambda(0) = I_{\lambda,0} e^{-\tau_{\lambda,0}} - \int_{\tau_{\lambda,0}}^0 S_\lambda e^{-\tau_\lambda} d\tau_\lambda \quad (4.17)$$

where  $I_{\lambda,0}$  is the initial intensity. Now, if we make the assumption of a plane parallel atmosphere and replace  $\tau_\lambda$  with  $\tau_{v,\lambda}$ , take initial position of the rays to be at  $\tau_{v,0} = \infty$  and drop the  $\lambda$  subscripts for simplicity, we get

$$I(0) = \int_0^\infty S \sec \theta e^{-\tau_v \sec \theta} d\tau_v \quad (4.18)$$

If we assume  $S = a + b\tau_v$ , then the above equation takes the form

$$I_\lambda(0) = a_\lambda + b_\lambda \cos \theta \quad (4.19)$$

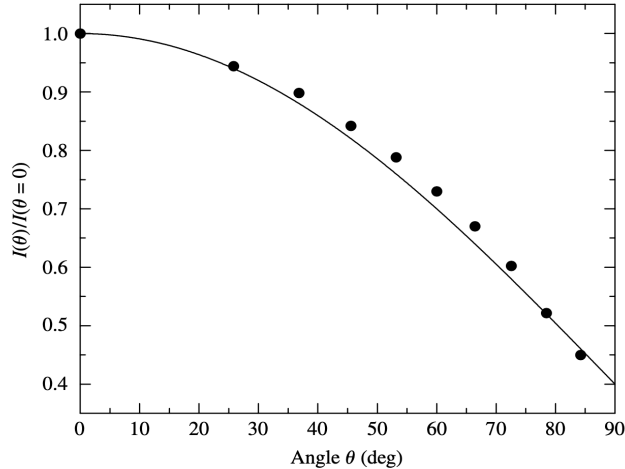


Figure 4.3: A theoretical Eddington approximation of solar limb darkening for light integrated over all wavelengths. The dots are observational data for the Sun [1].

If we use the Eddington approximation and the result we obtained in Eq. 4.15 and solve for the Sun we get a pretty close match with the observational data obtained for the Sun as shown in the figure above.

# Chapter 5

## The Sun

Due to its proximity to us, the star for which we have the greatest amount of observational data is our Sun. The tremendous wealth of information provided by the data serve as rigorous tests of our understanding of the physical processes operating within stellar atmospheres and interiors. In this section we will only go into the solar neutrino problem, the Parker solar wind model, the hydrodynamic nature of the upper solar atmosphere, magnetohydrodynamics and the solar cycle.

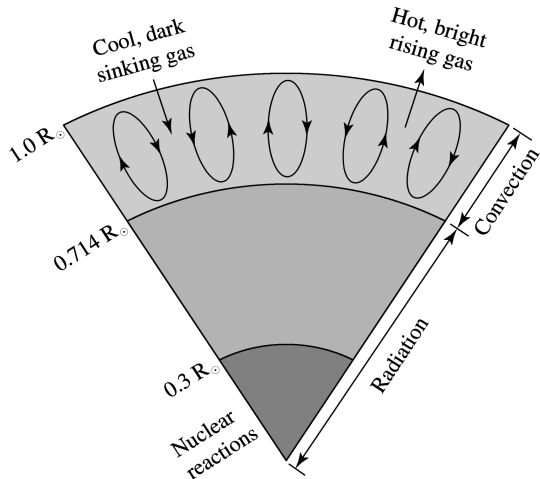


Figure 5.1: Schematic diagram of the Sun’s interior [1].

### 5.1 The Solar Neutrino Problem

Neutrinos are produced in different stages of the pp chain reaction in the solar interior. A discrepancy existed for decades between the predicted values of neutrino counts that should be detected on Earth, based on the solar model, and the actual neutrino counts that were detected by various neutrino observatories around the world. The actual neutrino counts were always significantly lesser than the predicted values.

The only logical explanation to this was either the solar model was fundamentally wrong or something was happening to the neutrinos on their way to Earth. An elegant solution to the solar neutrino problem proposed that the solar model is essentially correct but that the neutrinos produced in the Sun’s core actually change before they reach Earth. The Mikheyev–Smirnov–Wolfenstein (or MSW)

effect involves the transformation of neutrinos from one type to another.

The neutrinos produced in the various branches of the pp chain are all electron neutrinos ( $\nu_e$ ); however, two other flavors of neutrinos also exist—the muon neutrino ( $\nu_\mu$ ) and the tau neutrino ( $\nu_\tau$ ). The MSW effect suggests that neutrinos oscillate among flavors, being electron neutrinos, muon neutrinos, and/or tau neutrinos during their passage through the Sun. The neutrino oscillations are caused by interactions with electrons as the neutrinos travel toward the surface

## 5.2 The Parker Solar Wind Model

This model assumes that the solar corona is in hydrostatic equilibrium, is isothermal and has a negligible mass compared to the mass of the sun. With this, the condition for hydrostatic equilibrium gives us

$$\frac{dP}{dr} = -\frac{GM_\odot \rho}{r^2} \quad (5.1)$$

where  $M_\odot$  is the mass of the Sun. If we assume all of the gas to be made up of hydrogen which is completely ionised, take no. density as  $n = \rho/m_p$  and  $m_p \approx m_n$ , we get

$$P = 2nkT \quad (5.2)$$

according to the ideal gas law, where  $\mu = 1/2$  for ionised hydrogen.

Combining the above two equations and integrating, we get

$$n(r) = n_0 e^{-\lambda(1-r_0/r)} \quad (5.3)$$

where

$$\lambda \equiv \frac{GM_\odot n m_p}{2kTr_0}$$

which can also be written as

$$P(r) = P_0 e^{-\lambda(1-r_0/r)} \quad (5.4)$$

where  $P_0$  is the pressure at some  $r_0$ .

Plugging in the necessary constants in the equation and calculating  $P(\infty)$ , we get  $P(\infty) \simeq 5 \times 10^{-6}$ . However, with the exception of localized clouds of material, the actual densities and pressures of interstellar dust and gas are much lower than those just derived. As the assumption about the corona being isothermal is roughly consistent with observations, the assumption that the solar corona is in hydrostatic equilibrium must be wrong. Since  $P(\infty)$  greatly exceeds the pressures in interstellar space, material must be expanding outward from the Sun, implying the existence of the solar wind.

The existence of the solar wind has an important implication. As the Sun rotates and the solar wind ejects mass outward, there is a net torque opposing the rotation. The solar wind transfers angular momentum away from the Sun, slowing down its speed of rotation.

## 5.3 Hydrodynamic nature of the upper solar atmosphere

The following hydrodynamic equations help us in describing the outer atmosphere, as it is not in hydrostatic equilibrium.

$$\rho v \frac{dv}{dr} = -\frac{dP}{dr} = -\frac{GM_r \rho}{r^2} \quad (5.5)$$

where  $M_r$  is the mass that is enclosed by a sphere of radius  $r$ . Based on the fact that loss rate of mass is constant, we also have

$$4\pi r^2 \rho v = \text{const} \implies \frac{d}{dr} (\rho v r^2) = 0 \quad (5.6)$$

At the top of the convection zone, rising and falling gas sets up longitudinal waves (pressure waves) that propagate outward through the photosphere and the chromosphere.

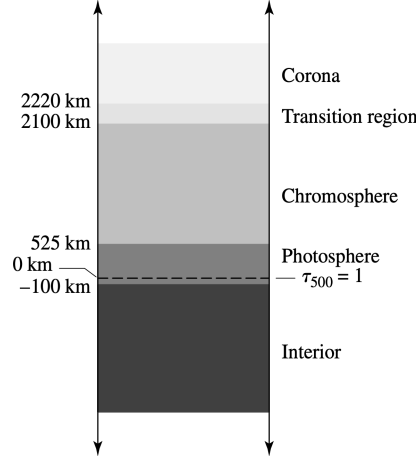


Figure 5.2: The components of the Sun's atmosphere [1].

The outward flux of wave energy  $F_E$ , is governed by the equation

$$F_E = \frac{1}{2} \rho v_w^2 v_s \quad (5.7)$$

where  $v_s$  is the local sound speed and  $v_w$  is the velocity amplitude of the oscillatory wave motion for individual particles being driven about their equilibrium positions by the “piston” of the convection zone.

$$v_s = \sqrt{\frac{\gamma P}{\rho}} = \sqrt{\frac{\gamma kT}{\mu m_H}} \propto \sqrt{T} \quad (5.8)$$

From photosphere to chromosphere,  $T$  does not change much. Hence  $v_s$  is almost the same. If we assume negligible loss of mechanical energy ( $F_E(4\pi r^2) = \text{constant}$ ), a significant drop in  $\rho$  means  $v_w$  has to increase according to Eq. 5.7. When  $v_w > v_s$ , the waves become supersonic, causing shockwaves that dissipate energy in the chromosphere. Through this mechanism, the upper layers of the Sun's atmosphere get heated up due to convection in the interior.

## 5.4 Magnetohydrodynamics (MHD) and Alfvén waves

The magnetic energy density  $u_m$  and magnetic pressure  $P_m$  are numerically equal and are given by

$$u_m = \frac{B^2}{2\mu_0} = P_m \quad (5.9)$$

Now, if a volume  $V$  of plasma containing a number of magnetic field lines is compressed perpendicular to the lines, the density of field lines necessarily increases. Hence, magnetic energy increases

by an amount equal to the external work done. This also means that there is a magnetic pressure developed which works to counteract the displacement caused. This is the “restoring force” that can set up oscillations and waves in the medium. These transverse MHD waves that are set up are called Alfvén waves.

The speed of propagation of the Alfvén wave may be estimated by making a comparison with the sound speed in a gas. Hence,

$$v_m \sim \sqrt{\frac{P_m}{\rho}} = \frac{B}{\sqrt{2\mu_0\rho}} \quad (5.10)$$

But, a more careful treatment gives

$$v_m = \frac{B}{\mu_0\rho} \quad (5.11)$$

According to Maxwell’s equations, a time-varying magnetic field produces an electric field, which in turn creates electrical currents in the highly conductive plasma. This implies that some resistive Joule heating will occur in the ionised gas due to Alfvén waves, causing the temperature to rise. Thus MHD waves contribute to the temperature structure of the upper solar atmosphere.

## 5.5 The Solar Cycle

The overall magnetic field of the Sun reverses every 11 years. This is linked with the sunspot cycle which also shows 11 year patterns.

### 5.5.1 Sunspots

Sunspots occur in regions of very high magnetic field strengths with the magnetic field lines themselves coming out of the surface of the Sun. It is believed that the existence of such intense magnetic fields “freezes” the plasma in the convection zone, inhibiting the energy transport outward, explaining why sunspots appear dark.

As part of the cycle which lasts 22 years, the sunspots first appear in higher latitudes and then start appearing at lower and lower latitudes until they meet at the equator (a period of around 11 years). Each sunspot lasts for a few months and is of the opposite polarity as the one preceding it. Following this there is a global magnetic field reversal of the Sun and the next sunspot that again appears at the higher latitude is of opposite polarity to the first sunspot that had appeared there 11 years ago. Thus a cycle of about 22 years is established.

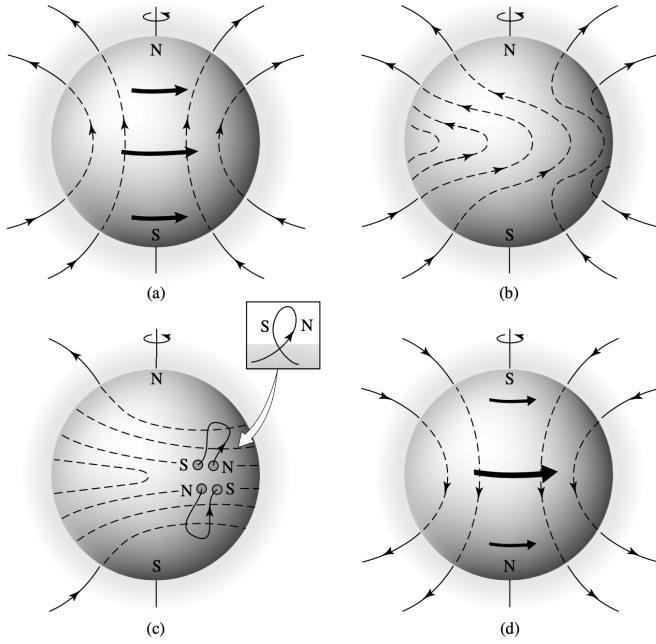


Figure 5.3: The Magnetic dynamo model of the Solar Cycle [1].

### 5.5.2 The Magnetic Dynamo Model

As depicted in the figure above, because the magnetic field lines are “frozen into” the gas, the differential rotation of the Sun drags the lines along, converting a poloidal field (essentially a simple magnetic dipole) to one that has a significant toroidal component (field lines that are wrapped around the Sun). The turbulent convection zone then has the effect of twisting the lines, creating regions of intense magnetic fields, called magnetic ropes. The buoyancy produced by magnetic pressure (Eq. 6.5) causes the ropes to rise to the surface, appearing as sunspot groups. The polarity of the sunspots is due to the direction of the magnetic field along the ropes; consequently, every lead spot in one hemisphere will have the same polarity while the lead spots in the other hemisphere will have the opposite polarity. Finally, the cancellation of magnetic fields near the equator causes the poloidal field to be reestablished, but with its original polarity reversed. This process takes approximately 11 years.

# Chapter 6

## Interior of Stars

In this chapter we aim to understand the physics that sanctions the existence of stars. We will see the forces that play a role in keeping stars from collapsing or expanding and also the fundamental processes that result in a star's massive energy output. We will also gradually build up on some stellar models based on these fundamental physics principles.

### 6.1 Hydrostatic Equilibrium and Mass conservation

To derive the condition for hydrostatic equilibrium in stellar interiors, we consider the following equation from Newton's second law for a spherically symmetric star (See fig 6.1).

$$dm \frac{d^2r}{dt^2} = F_g + F_{P,t} + F_{P,b} \implies dm \frac{d^2r}{dt^2} = F_g - dF_P \quad (6.1)$$

Now, writing  $F_g = -G \frac{M_r dm}{r^2}$ ,  $dm = \rho Adr$  and  $dF_p = AdP$ , we have

$$\rho \frac{d^2r}{dt^2} = -G \frac{M_r \rho}{r^2} - \frac{dP}{dr} \quad (6.2)$$

If the star is static, the acceleration must be zero. Hence,

$$\frac{dP}{dr} = -G \frac{M_r \rho}{r^2} = -\rho g \quad (6.3)$$

Which is the required condition for hydrostatic equilibrium.

We also have the mass conservation equation

$$\frac{dM_r}{dr} = 4\pi r^2 \rho \quad (6.4)$$

which dictates how the interior mass of a star must change with distance from the center.

### 6.2 Pressure Equation of State

We now aim to describe the origin of the pressure term used in the previous subsection and establish a relation between pressure and other fundamental parameters of the material. From statistical physics, we have the following pressure integral

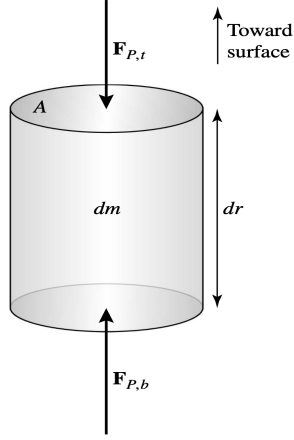


Figure 6.1: A cylindrical mass element in equilibrium in the star [1].

$$P = \frac{1}{3} \int_0^\infty n_p p v dp \quad (6.5)$$

which makes it possible to compute the pressure, given some distribution of  $n_p dp$ . The above equation is valid for both massive and massless particles. The ideal gas equation of state

$$P_g = \frac{\rho k T}{\mu m_H} \quad (6.6)$$

is a special result obtained from the above integral when the Maxwell-Boltzmann Distribution of  $n_p dp$  is substituted in it. In this form of the equation,  $\mu \equiv \bar{m}/m_H$  is the mean molecular weight and  $m_H$  is the mass of the hydrogen atom.

The mean molecular weights  $\mu_n$  and  $\mu_i$  for neutral and completely ionized gases respectively are given by

$$\begin{aligned} \frac{1}{\mu_n} &\simeq X + \frac{1}{4}Y + \left\langle \frac{1}{A} \right\rangle_n Z \\ \frac{1}{\mu_i} &\simeq 2X + \frac{3}{4}Y + \left\langle \frac{1+z}{A} \right\rangle_i Z \end{aligned} \quad (6.7)$$

where  $X, Y, Z$  are fractional abundances of hydrogen, helium and metals(elements heavier than helium) and  $z, A$  are the atomic and mass no.s respectively.

So far we have only seen the material contribution to pressure. The contribution due to radiation pressure can be derived by observing that

$$n_p dp = n_\nu d\nu \text{ and } P_\gamma = h\nu/c$$

Using this in eq. 6.5, we have

$$P_{rad} = \frac{1}{3} \int_0^\infty h\nu n_\nu d\nu = \frac{1}{3} \int_0^\infty u_\nu d\nu = \frac{1}{3} a T^4 \quad (6.8)$$

where the results from the Planck function for blackbody radiation have been used. Combining the two pressures, we have

$$P_t = \frac{\rho kT}{\mu m_H} + \frac{1}{3} a T^4 \quad (6.9)$$

## 6.3 Stellar Energy Sources

### 6.3.1 Timescales

If the source of stellar luminosity is assumed to be the loss of gravitational potential energy (a result of stellar collapse), a rough estimate of the star's age can be made. Assuming the star to be a sphere of constant density, its gravitational potential energy is given by

$$U_g \sim -\frac{3}{5} \frac{GM^2}{R}$$

According to the virial theorem, the total mechanical energy of the star is

$$E \sim -\frac{3}{10} \frac{GM^2}{R} \quad (6.10)$$

If we assume that initially the total energy of the star was zero as it was spread out across space infinitely, and also assume that the luminosity  $L$  of the star was a constant throughout this time, the time taken for the star to reach the current state is given by

$$t_{KH} = \frac{\Delta E_g}{L} = \frac{3}{10} \frac{GM^2}{LR} \quad (6.11)$$

This time is called the Kelvin-Helmholtz timescale. For the sun this time comes out to be  $t_{KH} \sim 10^7$  yr, which is far lesser than the age of the earth itself! Therefore, gravitational potential energy alone cannot account for the Sun's luminosity throughout its entire lifetime.

Now we will see if nuclear binding energy can act as fuel for stars. For simplicity, assume that the Sun was originally 100

$$E_{nuclear} = 0.1 \times 0.007 \times M_\odot c^2 = 1.3 \times 10^{44} J$$

This gives a nuclear timescale of approximately

$$t_{nuclear} = \frac{E_{nuclear}}{L_\odot} \sim 10^{10} \text{ yr} \quad (6.12)$$

more than enough time to account for the age of the earth.

### 6.3.2 Quantum Tunneling

For a nuclear reaction to occur, the nuclei of atoms must collide, forming new nuclei in the process. However, all nuclei are positively charged, meaning that a Coulomb potential energy barrier must be overcome before contact can occur as shown.

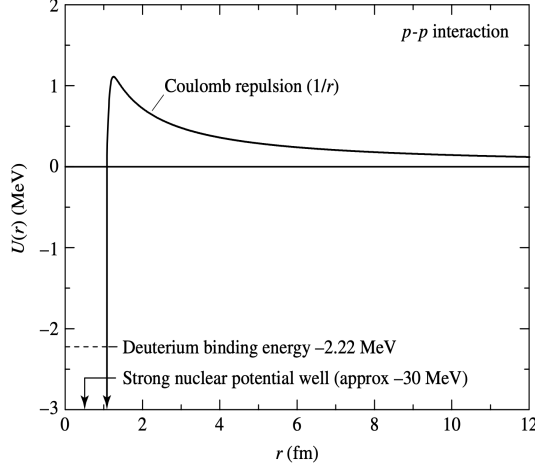


Figure 6.2: The potential energy curve characteristic of nuclear reactions. The nuclear potential well inside the nucleus is due to the attractive strong nuclear force. [1].

If we assume that the energy required to overcome the Coulomb barrier is provided by the thermal energy of the gas, and that all nuclei are moving nonrelativistically, then the temperature  $T_{classical}$  required to overcome the barrier can be estimated.

$$\frac{1}{2}\mu_m v^2 = \frac{3}{2}kT_{classical} = \frac{1}{4\pi\epsilon_0} \frac{Z_1 Z_2 e^2}{r}$$

where  $Z_1$  and  $Z_2$  are the numbers of protons in each nucleus, and  $r$  is their distance of separation. Assuming that the radius of a typical nucleus is on the order of  $1 \text{ fm} = 10^{-15} \text{ m}$ , the temperature needed to overcome the Coulomb potential energy barrier is approximately

$$T_{classical} = \frac{Z_1 Z_2 e^2}{6\pi\epsilon_0 kr} \sim 10^{10} \text{ K} \quad (6.13)$$

for a collision between two protons. However, the central temperature of the sun is only  $1.5 \times 10^7 \text{ K}$ , much lower than the required temperature. To overcome this problem, we need to take a look at the phenomenon of Quantum tunneling. The Heisenberg Uncertainty principle tells us that

$$\Delta x \Delta p_x \geq \frac{\hbar}{2} \quad (6.14)$$

As a crude estimate of the effect of tunneling on the temperature necessary to sustain nuclear reactions, assume that a proton must be within approximately one de Broglie wavelength of its target in order to tunnel through the Coulomb barrier. We have

$$\frac{1}{4\pi\epsilon_0} \frac{Z_1 Z_2 e^2}{\lambda} = \frac{p^2}{2\mu_m} = \frac{(h/\lambda)^2}{2\mu_m}$$

Solving for  $\lambda$  and substituting in place of  $r$  in eq. 6.13, we have

$$T_{quantum} = \frac{Z_1^2 Z_2^2 e^4 \mu_m}{12\pi^2 \epsilon_0^2 h^2 k} \sim 10^7 \text{ K} \quad (6.15)$$

which is consistent with the central temperatures of the Sun.

### 6.3.3 Nuclear Reaction Rates and the Gamow Peak

From statistical physics it is possible to derive that the number of reactions per unit volume, per unit time is

$$r_{ix} = \int_0^\infty n_x n_i \sigma(E) v(E) \frac{n_E}{n} dE \quad (6.16)$$

where  $n_x$  is the no. of targets per unit volume,  $n_i$  is no. of incident targets per unit volume,  $n_E dE$  is the Maxwell-Boltzmann distribution for particles,  $n$  is the total no. of particles per unit volume and  $\sigma(E)$  is the statistical cross section defined as the number of reactions per target nucleus per unit time, divided by the flux of incident particles.

A functional form of  $\sigma(E)$  can be derived by noticing that it is proportional to the actual cross sectional area of the target nucleus and the tunneling probability. The size of a nucleus, measured in terms of its ability to “touch” target nuclei, is approximately one de Broglie wavelength in radius ( $r \sim \lambda$ ).

$$\sigma(E) \propto \pi \lambda^2 \propto \pi (h/p)^2 \propto 1/E$$

Factoring in the tunneling probability using quantum mechanics,

$$\sigma(E) \propto e^{-bE^{-1/2}}$$

where

$$b \equiv \frac{\pi \mu_m^{1/2} Z_1 Z_2 e^2}{2^{1/2} \epsilon_0 h}$$

Thus we have,

$$\sigma(E) = \frac{S(E)}{E} e^{-bE^{-1/2}} \quad (6.17)$$

where  $S(E)$  is assumed to be some slowly varying function of energy. Upon substituting all the variables in eq. 6.16, we get

$$r_{ix} = \left( \frac{2}{kT} \right)^{3/2} \frac{n_i n_x}{(\mu_m \pi)^{1/2}} \int_0^\infty S(E) e^{-bE^{-1/2}} e^{-E/kT} dE \quad (6.18)$$

When the product of the two exponential terms inside the integral are plotted as a function of energy we get a curve that peaks strongly for a particular value of energy. This maxima is called the Gamow peak (See fig 6.3) and this occurs at an energy of

$$E_0 = \left( \frac{bkT}{2} \right)^{2/3} \quad (6.19)$$

As a consequence of the Gamow peak, the greatest contribution to the reaction rate integral comes in a fairly narrow energy band.

### 6.3.4 Luminosity Gradient

It is often illuminating to write the complicated reaction rate equations in the form of a power law centered at a particular temperature. Neglecting the screening factor, in the case of a two-particle interaction, the reaction rate would become

$$r_{ix} \simeq r_0 X_i X_x \rho^{\alpha'} T^\beta \quad (6.20)$$

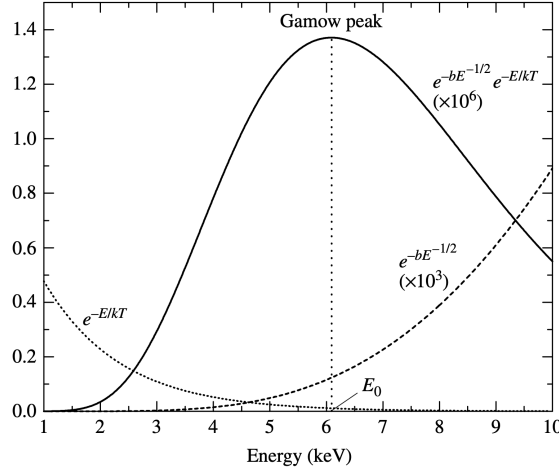


Figure 6.3: This particular example represents collisions of protons in the core of the Sun [1].

centered at a particular temperature, where  $X_i$  and  $X_x$  are the mass fractions of the two particles, and  $\alpha'$  and  $\beta$  are determined from the power law expansions of the reaction rate equations. If  $\varepsilon_0$  is the amount of energy released per reaction, the amount of energy liberated per kilogram of material per second becomes

$$\epsilon_{ix} = \left( \frac{\varepsilon_0}{\rho} \right) r_{ix}$$

The contribution to the total luminosity due to an infinitesimal mass  $dm$  is simply

$$dL = \epsilon dm \quad (6.21)$$

where  $\epsilon = \epsilon_{nuclear} + \epsilon_{gravity}$ . With this we have the luminosity gradient equation

$$\frac{dL_r}{dr} = 4\pi r^2 \rho \epsilon \quad (6.22)$$

where  $L_r$  is the interior luminosity due to all of the energy generated within the star's interior out to the radius  $r$ .

### 6.3.5 Stellar Nuclear reactions

Nuclear reactions obey a series of particle conservation laws i.e during every reaction it is necessary to conserve electric charge, the number of nucleons, and the number of leptons. The dominant groups of nuclear reactions occurring in stars are the Proton-Proton (PP) chains, the CNO Cycle, the triple alpha process of Helium burning and the Carbon-Oxygen burning chain reactions. Three of the energy generation rates per unit mass of substance are as follows:

$$\begin{aligned} \epsilon_{pp} &\simeq \epsilon'_{0pp} \rho X^2 f_{pp} \psi_{pp} C_{pp} T_6^4 \\ \epsilon_{CNO} &\simeq \epsilon'_{0CNO} \rho X X_{CNO} T_6^{19.9} \\ \epsilon_{3\alpha} &\simeq \epsilon'_{0,3\alpha} \rho^2 Y^3 f_{3\alpha} T_8^{41.0} \end{aligned} \quad (6.23)$$

where  $f$  is a screening factor,  $\psi$  and  $C$  are correction factors, and  $X$  and  $Y$  are the mass fractions of Hydrogen and Helium. The above equations are given to show the temperature dependence of the these processes.

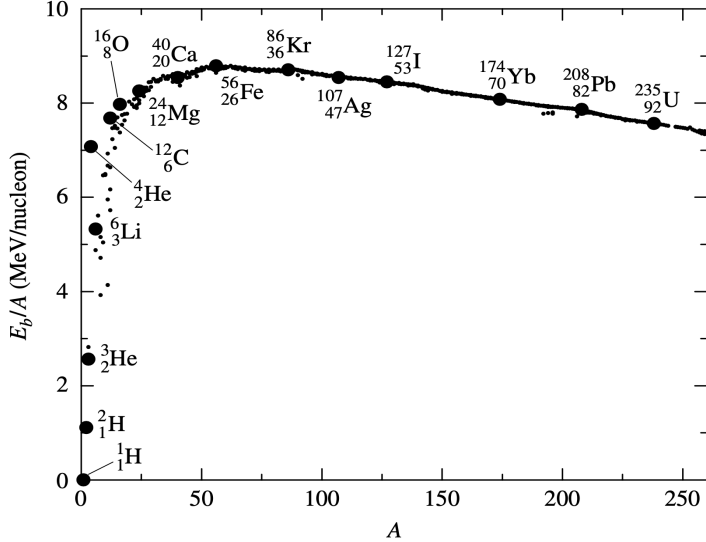


Figure 6.4: The binding energy per nucleon,  $E_b/A$ , as a function of mass number,  $A$  [1].

The ultimate result of successive chains of nuclear reactions within stars is the production of iron, assuming sufficient energy is available to overcome the Coulomb barrier. It is believed that shortly after the Big Bang the early universe was composed primarily of hydrogen and helium, with no heavy elements. Today, Earth and its inhabitants contain an abundance of heavier metals. The study of stellar nucleosynthesis strongly suggests that these heavier nuclei were generated in the interiors of stars. It can be said that we are all “star dust,” the product of heavy element generation within previous generations of stars.

## 6.4 Energy Transport and Thermodynamics

The three modes of energy transport in stellar interiors is radiation, convection and conduction, although conduction does not play a significant role.

### 6.4.1 The radiative temperature gradient

From stellar atmospheres, we know that

$$\frac{dP_{rad}}{dr} = -\frac{\bar{\kappa}\rho}{c}F_{rad}$$

From eq. 6.8, we also have

$$\frac{dP_{rad}}{dr} = \frac{4}{3}aT^3\frac{dT}{dr}$$

Combining these two equations and substituting the expression for  $F_{rad}$ , we have

$$\frac{dT}{dr} = -\frac{3}{4ac}\frac{\bar{\kappa}\rho}{T^3}\left(\frac{L_r}{4\pi r^2}\right) \quad (6.24)$$

### 6.4.2 The adiabatic temperature gradient

To describe convection, we first consider the situation where a hot convective bubble of gas rises and expands adiabatically, meaning that the bubble does not exchange heat with its surroundings. After it has traveled some distance, it finally thermalizes, giving up any excess heat as it loses its identity and dissolves into the surrounding gas.

Differentiating the ideal gas equation, we have

$$\frac{dP}{dr} = \frac{-P}{\mu} \frac{d\mu}{dr} + \frac{P}{\rho} \frac{dP}{dr} + \frac{P}{T} \frac{dT}{dr} \quad (6.25)$$

We also have

$$\frac{dP}{dr} = \frac{\gamma P}{\rho} \frac{dP}{dr} \quad (6.26)$$

from the adiabatic relation between pressure and density  $P = K\rho^\gamma$ . Combining the two equations, assuming  $\mu$  to be a constant, and using eq. 6.3 and the ideal gas law, we have

$$\left. \frac{dT}{dr} \right|_{ad} = -\left(1 - \frac{1}{\gamma}\right) \frac{\mu m_H}{k} \frac{GM_r}{r^2} \quad (6.27)$$

This result describes how the temperature of the gas inside the bubble changes as the bubble rises and expands adiabatically. If the star's actual temperature gradient (designated by the subscript *act*) is steeper than the adiabatic temperature gradient given in eq. 6.27, or

$$\left| \frac{dT}{dr} \right|_{act} > \left| \frac{dT}{dr} \right|_{ad}$$

the temperature gradient is said to be superadiabatic ( $dT/dr < 0$ ). It can be shown that this is in fact the criterion for convection to occur in the interior of stars (assuming  $\mu$  does not vary). An equivalent condition is

$$\frac{d \ln P}{d \ln T} < \frac{\gamma}{\gamma - 1} \quad (6.28)$$

For an ideal monoatomic gas,  $\gamma = 5/3$  and convection will occur in some region of a star when  $d \ln P / d \ln T < 2.5$ . In that case the temperature gradient ( $dT/dr$ ) is given approximately by eq. 6.27. When  $d \ln P / d \ln T > 2.5$ , the region is stable against convection and  $dT/dr$  is given by eq. 6.24.

### 6.4.3 Mixing Length Theory of superadiabatic convection

We define the pressure scale height, a characteristic length scale for convection, as follows

$$\frac{1}{H_P} \equiv -\frac{1}{P} \frac{dP}{dr} \quad (6.29)$$

Now we assume that a hot, rising bubble travels some distance

$$l = \alpha H_P \quad (6.30)$$

before dissipating, at which point it thermalizes with its surroundings, giving up its excess heat at constant pressure. The distance  $l$  is called the mixing length and  $\alpha$  is a free parameter.

$$\delta T = \left( \left. \frac{dT}{dr} \right|_{ad} - \left. \frac{dT}{dr} \right|_{act} \right) dr$$

The subscript 'ad' is for the bubble and 'act' is for the surroundings. After the bubble travels one mixing length, the excess heat flow per unit volume from bubble to surroundings is

$$\delta q = (C_P \delta T) \rho$$

The convective flux is given by  $F_c = \delta q \bar{v}_c$  where  $\bar{v}_c$  is the average velocity of the bubble as it travels the mixing length. Differentiating the ideal gas equation and setting  $\delta\mu$  and  $\delta P$  to zero (as we have assumed that the pressure of the bubble remains equal to the pressure of the surroundings at all times), we have

$$\delta\rho = -\frac{\rho}{T} \delta T$$

Thus the buoyant force per unit volume is

$$f_{net} = \frac{\rho g}{T} \delta T$$

Assuming  $\langle f_{net} \rangle = 1/2 f_{net}$ , equating work done by buoyant force to the kinetic energy gain of the bubble and solving for  $\bar{v}_c$  we have

$$\bar{v}_c = \left( \frac{2\beta \langle f_{net} \rangle l}{\rho} \right)^{1/2} \quad (6.31)$$

where  $\beta$  is a factor to account for the average value of  $v_c$ . With this we can solve for the convective flux to get

$$F_c = \rho C_P \left( \frac{k}{\mu m_H} \right)^2 \left( \frac{T}{g} \right)^{3/2} \beta^{1/2} \left[ \delta \left( \frac{dT}{dr} \right) \right]^{3/2} \alpha^2 \quad (6.32)$$

The derivation leading to the prescription for the convective flux given by eq. 6.32 is known as the mixing-length theory. Although basically a phenomenological theory containing arbitrary constants, the mixing-length theory is generally quite successful in predicting the results of observations. The equation when solved for difference in the temperature gradient and divided by the adiabatic temperature gradient gives us an estimate of how superadiabatic the temperature gradient must be to carry all of the flux by convection alone.

## 6.5 Stellar Model Building

The basic time independent stellar structure equations are summarized below.

$$\frac{dP}{dr} = -G \frac{M_r \rho}{r^2} \quad (6.3)$$

$$\frac{dM_r}{dr} = 4\pi r^2 \rho \quad (6.4)$$

$$\frac{dL_r}{dr} = 4\pi r^2 \rho \epsilon \quad (6.22)$$

$$\frac{dT}{dr} = -\frac{3}{4ac} \frac{\bar{\kappa} \rho}{T^3} \left( \frac{L_r}{4\pi r^2} \right) \quad (\text{radiation}) \quad (6.24)$$

$$= -\left( 1 - \frac{1}{\gamma} \right) \frac{\mu m_H}{k} \frac{GM_r}{r^2} \quad (\text{adiabatic convection}) \quad (6.27)$$

The last equation assumes that the convective temperature gradient is purely adiabatic and is applied when

$$\frac{d \ln P}{d \ln T} < \frac{\gamma}{\gamma - 1} \quad (6.28)$$

If the star is static, as assumed above, then  $\epsilon = \epsilon_{nuclear}$ . However, if the structure of the stellar model is changing over time, we must include the energy contribution due to gravity,  $\epsilon = \epsilon_{nuclear} + \epsilon_{gravity}$ .  $\epsilon_{gravity}$  can be related to entropy  $S$  as follows

$$\epsilon_{gravity} = -T \frac{dS}{dT} \quad (6.33)$$

### 6.5.1 Constitutive relations and Boundary Conditions

The basic stellar structure equations require information concerning the physical properties of the matter from which the star is made. Specifically, we need relationships for the pressure, the opacity, and the energy generation rate, in terms of fundamental characteristics of the material: the density, temperature, and composition. In general,

$$P = P(\rho, T, composition) \quad (6.34)$$

$$\bar{\kappa} = \bar{\kappa}(\rho, T, composition) \quad (6.35)$$

$$\epsilon = \epsilon(\rho, T, composition) \quad (6.36)$$

Boundary conditions play the essential role of defining the limits of integration. The central boundary conditions are fairly obvious—namely that the interior mass and luminosity must approach zero at the center of the star. A second set of boundary conditions is required at the surface of the star. The simplest set of assumptions is that the temperature, pressure, and density all approach zero at some surface value for the star's radius,  $R_*$ . With this the above differential equations are numerically integrated to get stellar parameters at different depths.

**Vogt-Russell Theorem:** The mass and the composition structure throughout a star uniquely determine its radius, luminosity, and internal structure, as well as its subsequent evolution. The dependence of a star's evolution on mass and composition is a consequence of the change in composition due to nuclear burning.

### 6.5.2 Lane-Emden Equations and Polytropic Models

Under very special and restrictive situations, it is possible to find analytic solutions to a subset of the stellar structure equations. Hypothetical stellar models in which the pressure depends on density in the form  $P = K\rho^\gamma$  are known as polytropes. Differentiating eq. 6.3 and substituting eq. 6.4 into this equation we get a Poisson's differential equation.

$$\frac{1}{r^2} \frac{d}{dr} \left( \frac{r^2}{\rho} \frac{dP}{dr} \right) = -4\pi G\rho \quad (6.37)$$

Now, we use the relation  $P(\rho) = K\rho^\gamma$ , write  $\gamma \equiv (n+1)/n$ , where  $n$  is the polytropic index, and write

$$\rho(r) \equiv \rho_c [D_n(r)]^n \quad \text{where } 0 \leq D_n \leq 1$$

where  $\rho_c$  is the central density of the model to get

$$\left[ (n+1) \left( \frac{K\rho_c^{(1-n)/n}}{4\pi G} \right) \right] \frac{1}{r^2} \frac{d}{dr} \left[ r^2 \frac{dD_n}{dr} \right] = -D_n^n$$

Defining

$$\lambda_n \equiv \left[ (n+1) \left( \frac{K \rho_c^{(1-n)/n}}{4\pi G} \right) \right]$$

and introducing the dimensionless independent variable  $\xi$  via

$$r \equiv \lambda_n \xi$$

we get the famous Lane-Emden equation.

$$\frac{1}{\xi^2} \frac{d}{d\xi} \left[ \xi^2 \frac{dD_n}{d\xi} \right] = -D_n^n \quad (6.38)$$

Solving this differential equation requires two boundary conditions. Assuming that the “surface” of the star is that location where the pressure goes to zero (and correspondingly the density of the gas also goes to zero), then

$$D_n(\xi_1) = 0 \text{ specifies the surface at } \xi = \xi_1$$

The second boundary condition is a consequence of eq. 6.3 and the polytropic equation which tells us that

$$\frac{dD_n}{d\xi} = 0 \text{ at } \xi = 0$$

Solving the equation gives us the density profile, which in turn gives us the pressure profile, which in turn gives us the temperature profile from the ideal gas equation. With the density profile known, the mass of the star also can be analytically obtained as

$$M = -4\pi \lambda_n^3 \rho_c \xi_1^2 \frac{dD_n}{d\xi} \Big|_{\xi_1} \quad (6.39)$$

There only three analytical solutions to the Lane-Emden equations i.e for  $n = 0, 1, 5$ . For polytropic indices of  $n > 5$  the mass contained in the star goes to infinity as the radius goes to infinity. Hence, the physically important indices are those that lie in between 0 and 5.  $n = 1.5$  corresponds to an ideal, monoatomic gas described under adiabatic processes. Another important polytropic index is the  $n = 3$  “Eddington standard model” associated with a star in radiative equilibrium (the equation can be solved numerically for these indices).

## 6.6 Main Sequence and Eddington Luminosity limit

If the temperature is sufficiently high and the gas density is low enough, it is possible for radiation pressure to dominate over the gas pressure in certain regions of the star, a situation that can occur in the outer layers of very massive stars. From stellar atmospheres we have

$$\frac{dP}{dr} \simeq \frac{\bar{\kappa}\rho}{c} \frac{L}{4\pi r^2} \quad (6.40)$$

Combining this with eq. 6.3 at the surface, we have

$$L_{Ed} = \frac{4\pi G c}{\bar{\kappa}} M \quad (6.41)$$

$L_{Ed}$  or the Eddington Limit is the maximum radiative luminosity that a star can have and still remain in hydrostatic equilibrium. This is the required mass-luminosity relation for main-sequence stars. (Stars undergoing hydrogen burning in their cores lie along the observational main sequence).

# Chapter 7

## Star Formation

### 7.1 Formation of protostars

#### 7.1.1 Jeans Criterion

One area where the picture is far from complete is in the earliest stage of evolution, the formation of pre-nuclear-burning objects known as protostars from interstellar molecular clouds. If globules and cores in molecular clouds are the sites of star formation, what conditions must exist for collapse to occur? The virial theorem,

$$2K + U = 0 \quad (7.1)$$

describes the condition of equilibrium for a stable, gravitationally bound system. If twice the total internal kinetic energy of a molecular cloud ( $2K$ ) exceeds the absolute value of the gravitational potential energy ( $|U|$ ), the force due to the gas pressure will dominate the force of gravity and the cloud will expand. On the other hand, if the internal kinetic energy is too low, the cloud will collapse. The boundary between these two cases describes the critical condition for stability when rotation, turbulence, and magnetic fields are neglected.

Assuming a spherical cloud of constant density, the gravitational potential energy is approximately

$$U_g \sim -\frac{3}{5} \frac{GM^2}{R}$$

where  $M_c$  and  $R_c$  are the mass and radius of the cloud. The cloud's internal kinetic energy, given by

$$K = \frac{3}{2} N k T$$

where  $N$  is the total no. of particles given by  $M_c/\mu m_H$ . Thus the condition for collapse is

$$\frac{3M_c k T}{\mu m_H} < \frac{3}{5} \frac{GM^2}{R} \quad (7.2)$$

Relating radius to the mass assuming a constant density of  $\rho_0$  throughout the cloud, we may solve for the minimum mass necessary to initiate spontaneous collapse. This is the Jeans criterion

$$M_c > M_J$$

where

$$M_J \simeq \left( \frac{5kT}{G\mu m_H} \right)^{3/2} \left( \frac{3}{4\pi\rho_0} \right) \quad (7.3)$$

where  $M_J$  is called the Jeans mass. The Jeans mass derivation given above neglected the important fact that there must exist an external pressure on the cloud due to the surrounding interstellar medium. If we include this, the critical mass required for gravitational collapse in the presence of an external gas pressure of  $P_0$  is given by the Bonnor–Ebert mass,

$$M_{BE} = \frac{c_{BE} v_T^4}{P_0^{1/4} G^{3/2}} \quad (7.4)$$

where  $v_T \equiv \sqrt{kT/\mu m_H}$  is the isothermal sound speed and the dimensionless constant  $c_{BE} \simeq 1.18$ .

### 7.1.2 Homologous Collapse

In the case that the criterion for gravitational collapse has been satisfied in the absence of rotation, turbulence, or magnetic fields, the molecular cloud will collapse. The collapse for the most part is isothermal as the gravitational potential energy is radiated away through the optically thin cloud. If we assume the pressure gradient to be negligible throughout the cloud, from the spherically symmetric hydrodynamic equation, we have

$$\frac{d^2r}{dt^2} = -\frac{GM_r}{r^2} \quad (7.5)$$

Since we are interested only in a surface that enclose mass  $M_r$  and noting that this internal mass remains constant throughout the collapse, we replace  $M_r$  with  $4/3\pi\rho_0 r_0^3$  where  $\rho$  and  $r_0$  are initial quantities. Multiplying the equation with the velocity of the surface allows us to integrate once along with the initial condition of  $dr/dt = 0$ , when  $r = r_0$ , to get the velocity of the surface.

$$\frac{dr}{dt} = -\left[\frac{8\pi}{3}G\rho_0 r_0^2 \left(\frac{r}{r_0} - 1\right)\right]^{1/2} \quad (7.6)$$

To integrate this equation, we make the substitutions

$$\cos^2 \xi \equiv r/r_0$$

and

$$\chi \equiv \left(\frac{8\pi}{3}G\rho_0\right)$$

to get

$$\cos^2 \xi \frac{d\xi}{dt} = \frac{\chi}{2} \quad (7.7)$$

which can be integrated with the initial condition that  $r = r_0$  when  $t = 0$  to get

$$\xi + \frac{1}{2} \sin 2\xi = \chi t \quad (7.8)$$

which is the equation of motion of the surface of a gravitationally collapsing cloud in parameterized form. With this it is possible to derive the free-fall timescale  $t_{ff}$ , when the radius of the collapsing sphere reaches zero.

$$t_{ff} = \left(\frac{3\pi}{32} \frac{1}{G\rho_0}\right)^{1/2} \quad (7.9)$$

Note that this does not depend on the initial size of the cloud. However, if the cloud is somewhat centrally condensed when the collapse begins, the free-fall time will be shorter for material near the center than for material farther out. This is called an inside-out collapse.

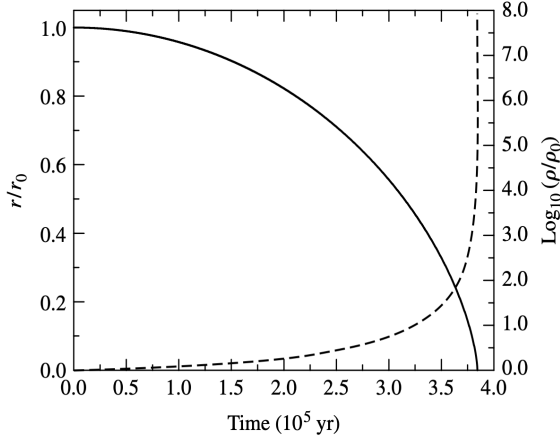


Figure 7.1: The homologous collapse of a molecular cloud.  $r/r_0$  is shown as the solid line and  $\log_{10}(\rho/\rho_0)$  is shown as the dashed line. [1].

### 7.1.3 Fragmentation of Collapsing Clouds

Since the masses of fairly large molecular clouds could exceed the Jeans limit, from eq. 7.3 our simple analysis seems to imply that stars can form with very large masses, possibly up to the initial mass of the cloud. However, this does not happen and stars frequently (perhaps even preferentially) tend to form in groups, ranging from binary star systems to clusters that contain hundreds of thousands of members.

An important consequence of the collapse of a molecular cloud is that the density of the cloud increases by many orders of magnitude during free-fall (Fig. 7.1). Consequently, since  $T$  remains nearly constant throughout much of the collapse, it appears that the Jeans mass must decrease. After collapse has begun, any initial inhomogeneities in density will cause individual sections of the cloud to satisfy the Jeans mass limit independently and begin to collapse locally, producing smaller features within the original cloud.

If the collapse changes from being essentially isothermal to adiabatic, the associated temperature rise would begin to affect the value of the Jeans mass. This is what stops the process of fragmentation. Using the adiabatic relation between density and temperature in the expression for Jeans mass, we have

$$M_J \propto \rho^{1/2} \quad (7.10)$$

for monoatomic hydrogen. Thus the Jeans mass increases with increasing density for a perfectly adiabatic collapse of a cloud. This behavior means that the collapse results in a minimum value for the mass of the fragments produced. By the virial theorem, the energy released is roughly

$$\Delta E_g \simeq \frac{3}{10} \frac{GM_J^2}{R_J}$$

Averaged over the free-fall time, the luminosity due to gravity is given by

$$L_{ff} \simeq \frac{\Delta E_g}{t_{ff}} \sim G^{3/2} \left( \frac{M_J}{R_J} \right)^{5/2}$$

where the terms of order of unity have been neglected. Since, the cloud is not a perfect blackbody, we may express the radiated luminosity as

$$L_{rad} = 4\pi R^2 e\sigma T^4$$

Equating the two and eliminating the radius we get the minimum obtainable Jeans mass, an estimate of when adiabatic effects become important.

$$M_{J_{min}} = 0.03 \left( \frac{T^{1/4}}{e^{1/2} \mu^{9/4}} \right) M_{\odot} \quad (7.11)$$

Fragmentation ceases when the segments of the original cloud begin to reach the range of solar mass objects.

#### 7.1.4 Additional processes in protostar formation

Important to the problem of the collapse process are the possible effects of rotation (angular momentum), the deviation from spherical symmetry, turbulent motions in the gas, and the presence of magnetic fields. For example, an appreciable amount of angular momentum present in the original cloud is likely to result in a disk-like structure for at least a part of the original material, since collapse will proceed at a more rapid rate along the axis of rotation relative to collapse along the equator.

Zeeman measurements of various molecular clouds indicate the presence of magnetic fields with strengths typically on the order of magnitude of 1 to 100 nT. If the magnetic field of a cloud is “frozen in,” and the cloud is compressed, the magnetic field strength will increase, leading to an increase in the magnetic pressure and resistance to the compression. In fact, if the cloud is stable to collapse because of magnetic pressure, it will remain so as long as the magnetic field does not decay.

When magnetic fields are included in the derivation of Jeans mass, we get the critical mass to be

$$M_B = \frac{c_B \pi R^2 B}{G^{1/2}} \quad (7.12)$$

where  $c_B = 380 N^{1/2} m^{-1} T^{-1}$ . Or

$$M_B \simeq 70 M_{\odot} \left( \frac{B}{1 \text{nT}} \right) \left( \frac{R}{1 \text{pc}} \right)^2 \quad (7.13)$$

## 7.2 Evolutionary Tracks

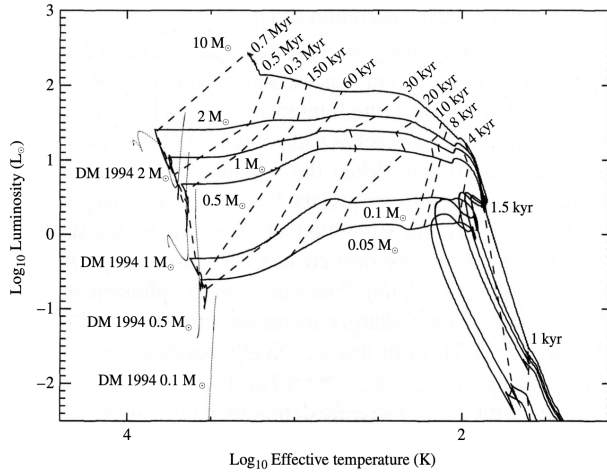


Figure 7.2: Theoretical evolutionary tracks. The dashed lines show time since collapse began [1].

Consider a spherical cloud of approximately  $1 M_{\odot}$  and solar composition that is super-critical and undergoing inside-out collapse. When the density of the material near the center of the collapse region reaches approximately  $10^{-10} \text{ kg/m}^3$ , the region becomes optically thick and the collapse becomes more adiabatic. The increased pressure that occurs when the collapse becomes adiabatic substantially slows the rate of collapse near the core. At this point the central region is nearly in hydrostatic equilibrium with a radius of approximately 5 AU. It is this central object that is referred to as a protostar.

Above the developing protostellar core, material is still in free-fall. When the infalling material meets the nearly hydrostatic core, a shock wave develops. It is at this shock front that the infalling material loses a significant fraction of its kinetic energy in the form of heat that “powers” the cloud and produces much of its luminosity.

When the temperature reaches approximately 1000 K, the dust within the developing protostar begins to vaporize and the opacity drops. Since the luminosity remains high during this phase, a corresponding increase in the effective temperature must occur. A second collapse occurs when the molecular hydrogen dissociates into atoms in the core absorbing the energy that would have been used to maintain hydrostatic equilibrium. After a second shock due to the infalling material, the core temperature has become high enough for deuterium burning to start. This is the constant luminosity part of the evolutionary track.

When deuterium burn-out occurs, the evolutionary track bends sharply downward and the effective temperature decreases slightly. The evolution has now reached a quasi-static pre-main-sequence phase.

### 7.3 Pre-main sequence evolution

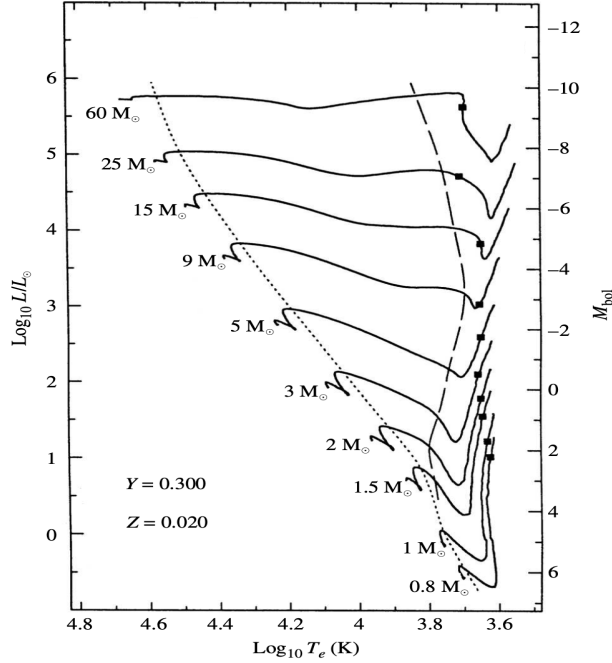


Figure 7.3: Classical pre-main-sequence evolutionary tracks computed for stars of various masses [1].

With the steadily increasing effective temperature of the protostar, the opacity of the outer lay-

ers becomes dominated by the  $\text{H}^-$  ion. This large opacity contribution causes the envelope of a contracting protostar to become convective. In fact, in some cases the convection zone extends all the way to the center of the star. The constraints convection puts on the structure of a star, a deep convective envelope limits its quasi-static evolutionary path to a line that is nearly vertical in the H–R diagram. Consequently, as the protostar collapse slows, its luminosity decreases while its effective temperature increases slightly. It is this evolution along the Hayashi track that appears as the downward turn at the end of the evolutionary tracks shown in Fig. 7.2.

As the central temperature continues to rise, increasing levels of ionization decrease the opacity in that region and a radiative core develops. At the point of minimum luminosity in the tracks following the descent along the Hayashi track, the existence of the radiative core allows energy to escape into the convective envelope more readily, causing the luminosity of the star to increase again. Also, the effective temperature continues to increase, since the star is still shrinking.

Now, the onset of the highly temperature dependent CNO cycle causes the core to become slightly convective which in turn causes the core to expand and the luminosity to drop. Following this, the star finally settles down onto the main sequence. The diagonal line in the H–R diagram where stars of various masses first reach the main sequence and begin equilibrium hydrogen burning is known as the zero-age main sequence.

# Chapter 8

## Main Sequence and Post Main Sequence evolution

Pre-main-sequence evolution is governed by the freefall timescale and the Kelvin-Helmholtz timescale, whereas main-sequence evolution is governed by the nuclear timescale. It is the difference in timescales for the various phases of evolution of individual stars that explains why approximately 80% to 90% of all stars in the solar neighborhood are observed to be main-sequence stars; we are more likely to find stars on the main sequence simply because that stage of evolution requires the most time; later stages of evolution proceed more rapidly.

### 8.1 Low-mass main-sequence evolution

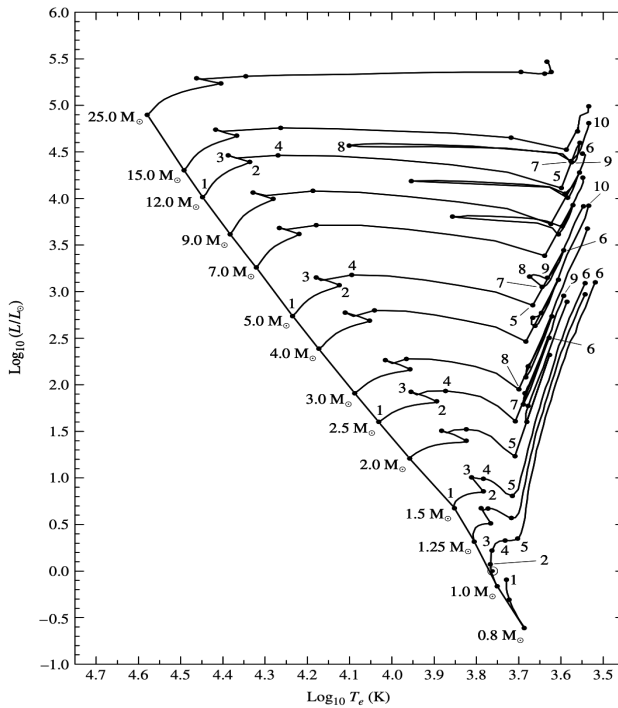


Figure 8.1: Main-sequence and post-main-sequence evolutionary tracks of stars [1].

The pp chain reaction that converts hydrogen to helium causes the mean molecular weight of the core to increase. From the ideal gas law, this should mean that the pressure holding up the overlying layers should decrease causing the core to compress, liberating energy through the loss of gravitational potential energy. This process causes the luminosity and the temperature to increase slowly.

With the depletion of hydrogen in the core, the generation of energy via the pp chain must stop. However, by now the core temperature has increased to the point that nuclear fusion continues to generate energy in a thick hydrogen-burning shell around a small, predominantly helium core. Since the luminosity is close to zero throughout the inner 3% of the star, the temperature gradient must also be zero resulting in an isothermal helium core.

At this point, the luminosity being generated in the thick shell actually exceeds what was produced by the core during the phase of core hydrogen burning. As a result, the evolutionary track continues to rise beyond point 3 in 8.1, although not all of the energy generated reaches the surface; some of it goes into a slow expansion of the envelope. Consequently, the effective temperature begins to decrease slightly and the evolutionary track bends to the right. As the hydrogen-burning shell continues to consume its nuclear fuel, the ash from nuclear burning causes the isothermal helium core to grow in mass while the star moves farther to the red in the H–R diagram.

## 8.2 Schönberg-Chandrashekhar limit

This phase of evolution ends when the mass of the isothermal core has become too great and the core is no longer capable of supporting the material above it. This mass is given by the Schönberg-Chandrashekhar limit. We start by dividing the equations of hydrostatic equilibrium and mass conservation to get

$$\frac{dP}{dM_r} = -\frac{GM_r}{4\pi r^4} \quad (8.1)$$

This can be rewritten in the form

$$\frac{d(4\pi r^3 P)}{dM_r} - \frac{3P}{\rho} = -\frac{GM_r}{r} \quad (8.2)$$

Rewriting  $P$  in the second term from the ideal gas equation and integrating over the mass of the isothermal core  $M_{ic}$ , we have

$$4\pi R_{ic}^3 P_{ic} - 2K_{ic} = U_{ic} \quad (8.3)$$

where  $K_{ic}$  is the total thermal energy of the core,  $U_{ic}$  is the gravitational potential energy of the core, and where we have taken temperature and mean molecular weight to be constant throughout the core. This is nothing but the generalized form of the virial theorem for stellar interiors in hydrostatic equilibrium.

Substituting the relevant expressions and solving for  $P_{ic}$ , we have

$$P_{ic} = \frac{3}{4\pi R_{ic}^3} \left( \frac{M_{ic} k T_{ic}}{\mu_{ic} m_H} - \frac{1}{5} \frac{GM_{ic}^2}{R_{ic}} \right) \quad (8.4)$$

Differentiating the expression with respect to  $M_{ic}$  and equating to zero we have

$$R_{ic} = \frac{2}{5} \frac{GM_{ic}\mu_{ic}m_H}{kT}$$

. Thus,

$$P_{ic,max} = \frac{375}{64\pi} \frac{1}{GM_{ic}^2} \left( \frac{kT_{ic}}{\mu_{ic} m_H} \right)^4 \quad (8.5)$$

As the core mass increases, the maximum pressure at the surface of the core decreases. At some point, it may no longer be possible for the core to support the overlying layers of the star's envelope. Clearly this critical condition must be related to the mass contained in the envelope and therefore to the total mass of the star.

The pressure of the overlying envelope can be estimated as

$$P_{ic,env} \sim \frac{81}{4\pi} \frac{1}{G^3 M^2} \left( \frac{kT_{ic}}{\mu_{env} m_H} \right)^4 \quad (8.6)$$

through some crude assumptions about density. Here  $\mu_{env}$  is the mean molecular weight of the envelope. Equating the two pressures we obtain the limit of the mass fraction of the isothermal core.

$$\frac{M_{ic}}{M} \sim 0.54 \left( \frac{\mu_{env}}{\mu_{ic}} \right)^2 \quad (8.7)$$

The expression originally obtained by the two scientists had a slightly smaller pre-factor of 0.37. The mass of an isothermal core may exceed the Schönberg–Chandrasekhar limit if an additional source of pressure can be found to supplement the ideal gas pressure. This can occur if the electrons in the gas start to become degenerate.

### 8.3 Post Main Sequence Evolution

Post main sequence evolution of low mass and intermediate mass stars can be summarized through the following plots.

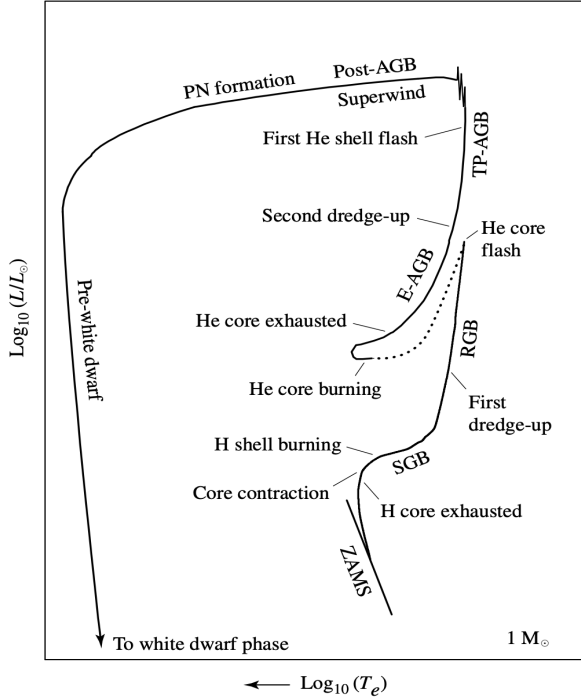


Figure 8.2: A schematic diagram of the evolution of a low-mass star of  $1 M_\odot$  from the zero-age main sequence to the formation of a white dwarf star [1].

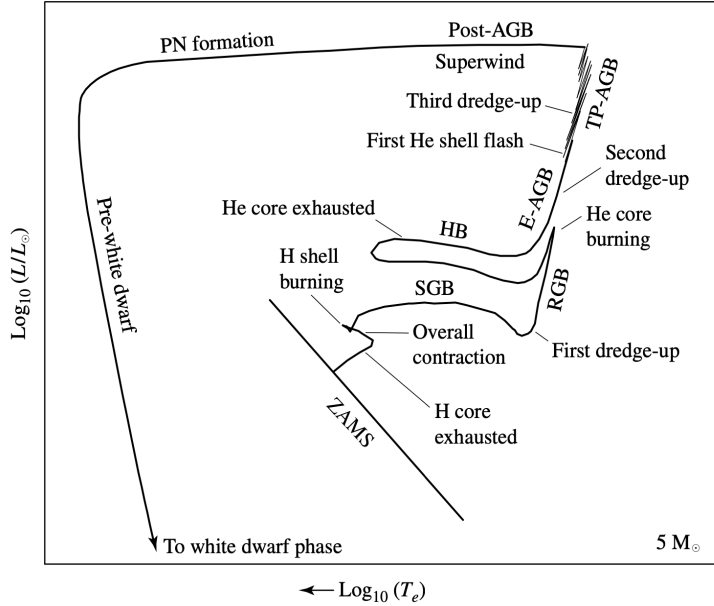


Figure 8.3: A schematic diagram of the evolution of an intermediate-mass star of  $5 M_{\odot}$  from the zero-age main sequence to the formation of a white dwarf star [1].

## 8.4 Helium core flash

An interesting difference arises after the Red Giant Branch (RGB) between the evolution of stars with masses greater than about  $1.8 M_{\odot}$  and those that have masses less than  $1.8 M_{\odot}$ . For stars of lower mass, as the helium core continues to collapse during evolution up to the tip of the red giant branch, the core becomes strongly electron-degenerate. Furthermore, significant neutrino losses from the core of the star prior to reaching the tip of the RGB result in a negative temperature gradient near the center (i.e., a temperature inversion develops); the core is actually refrigerated somewhat because of the energy that is carried away by the easily escaping neutrinos! When the temperature and density become high enough to initiate the triple alpha process, the ensuing energy release is almost explosive. The ignition of helium burning occurs initially in a shell around the center of the star, but the entire core quickly becomes involved and the temperature inversion is lifted. The luminosity generated by the helium-burning core reaches  $10^{11} L_{\odot}$ , comparable to that of an entire galaxy! However, this tremendous energy release lasts for only a few seconds, and most of the energy never even reaches the surface. Instead, it is absorbed by the overlying layers of the envelope.

# Chapter 9

## Stellar Pulsation

### 9.1 Period Luminosity relation

Pulsating stars are those stars that periodically dim and brighten as their surfaces expand and contract. It was noticed by astronomers that more luminous Cepheids (a class of pulsating stars) took longer to go through their pulsation cycles. With this observation the apparent magnitudes of these stars were plotted as a function of their pulsation periods.

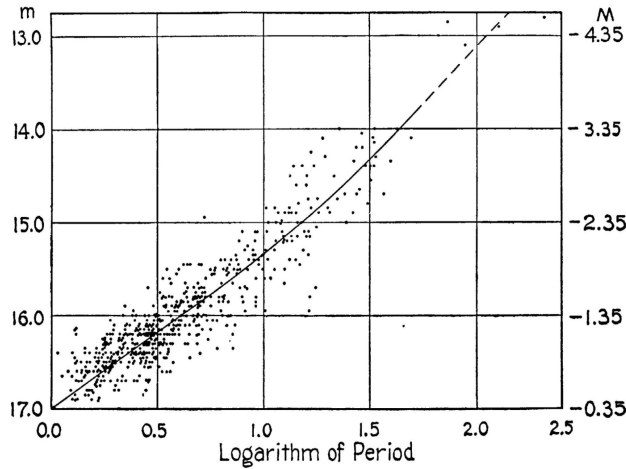


Figure 9.1: Classical Cepheids in the Small Magellanic Cloud with the period unit in days [1].

The calibrated period-luminosity relation for the V-band is given by

$$M_{(V)} = -2.81 \log_{10} P_d - 1.43 \quad (9.1)$$

where  $M_{(V)}$  is the absolute V magnitude and  $P_d$  is the pulsation period in days. Similarly the infrared H- band period luminosity fit and the period-luminosity-color relation fit is given by

$$H = 3.234 \log_{10} P_d + 16.079 \quad (9.2)$$

$$H = -3.428 \log_{10} P_d + 1.54 \langle J - K_s \rangle + 15.637 \quad (9.3)$$

where  $\langle J - K_s \rangle$  is the infrared color index.

## 9.2 Physics of Stellar Pulsation

### 9.2.1 Period-Density Relation

The radial oscillations of a pulsating star are the result of sound waves resonating in the star's interior. A rough estimate of the pulsation period may be obtained by considering how long it would take a sound wave to cross the diameter of a model star of radius  $R$  and constant density  $\rho$ .

$$\frac{dP}{dr} = -\frac{GM_r\rho}{r^2} = -\frac{4}{3}\pi G\rho^2 r$$

This is integrated with the boundary condition  $P = 0$  at the surface to get

$$P(r) = \frac{2}{3}\pi G\rho^2(R^2 - r^2) \quad (9.4)$$

Substituting this in the expression for the adiabatic sound speed, we have

$$\Pi \approx 2 \int_0^R \frac{dr}{v_s} \approx 2 \int_0^R \frac{dr}{\sqrt{\frac{2}{3}\gamma\pi G\rho(R^2 - r^2)}}$$

Solving this, we have

$$\Pi \approx \sqrt{\frac{3\pi}{2\gamma G\rho}} \quad (9.5)$$

which is in agreement with the periods of classical Cepheids.

Similar to standing waves in an open pipe, the pulsation in stellar interiors has different radial modes. The vast majority of stars oscillate in their fundamental mode or at the most their first overtone.

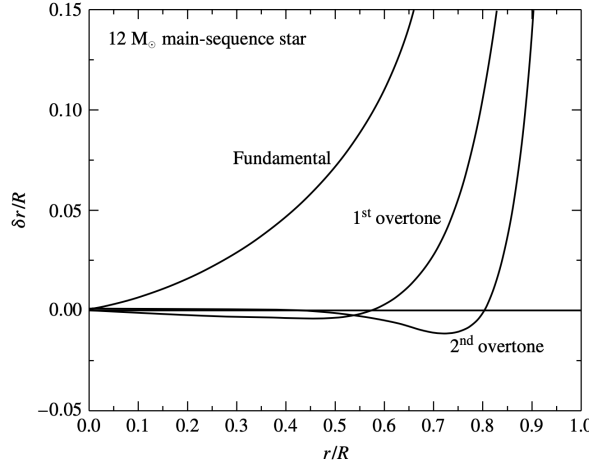


Figure 9.2: Radial modes of a pulsating star. This figure shows the fractional displacement  $\delta r/R$  of the stellar material from the equilibrium position [1].

### 9.2.2 The Eddington valve mechanism

To answer the question of what drives these oscillations, Eddington came up with a valve mechanism. If a layer of a star become more opaque upon compression, it could "dam up" the energy flowing

towards the surface and push the surface layers upward. The, as this expanding layer became more opaque, the trapped heat could escape and the layer could fall back down to begin the cycle anew. For this to work, *the opacity must increase with compression*. However, in most cases opacity decreases with compression. This is because the Kramer's law opacity  $\kappa$  is usually  $\kappa \propto \rho/T^{3.5}$ , which means it is more sensitive to temperature than density. As a layer is compressed, the density and temperature increase, resulting in an overall decrease in opacity.

The answer to this problem lies in the partial-ionization zones in stars. In these layers of the stars, part of the work done on the gases as they are compressed produces further ionization rather than raising the temperature of the gas. With a smaller temperature rise, the increase in compression causes a corresponding increase in Kramer's opacity. Similarly during expansion, the temperature does not decrease much as the ions recombine with the electrons, releasing energy. The location of these ionization zones within the star determine its pulsational properties.

### 9.3 Modeling Stellar Pulsation

We now consider an unrealistic, yet informative model of stellar pulsation called the one-zone model. According to this model, the star consists of a central point mass equal to the entire mass of the star  $M$ , surrounded by a single thin spherical shell or radius  $R$  and mass  $m$  representing the surface of the star. The interior of the shell is filled with a massless gas of pressure  $P$  whose sole function is to support the shell against the gravitational pull of the central mass  $M$ .

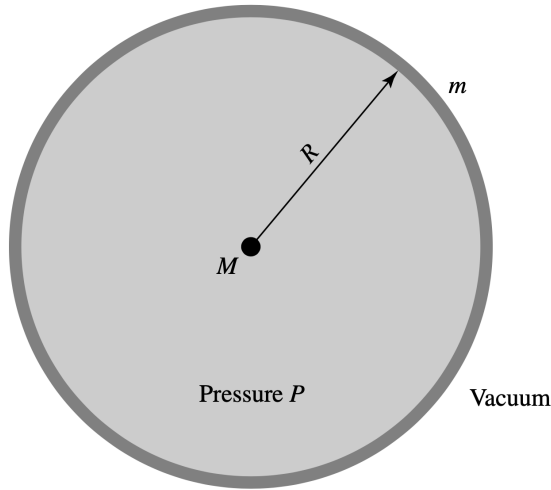


Figure 9.3: One-zone model of a pulsating star [1].

Newton's second law applied to the shell is

$$\rho \frac{d^2r}{dt^2} = -\frac{GM_r\rho}{r^2} - \frac{dP}{dr} \quad (9.6)$$

We now linearize radius and pressure, as the amplitude of oscillations is quite small.

$$R = R_0 + \delta R \text{ and } P = P_0 + \delta P$$

where  $R_0$  and  $P_0$  are equilibrium values. Substituting this into eq. 9.6 and using first-order approximations, we get

$$m \frac{d^2(\delta R)}{dt^2} = \frac{2GMm}{R_0^3} \delta R + 8\pi R_0 P_0 \delta R + 4\pi R_0^2 \delta P \quad (9.7)$$

We now assume our model to be adiabatic to get a relation between  $P$  and  $R$ , which is nothing but

$$PR^{3\gamma} = \text{const.}$$

The linearized version of this expression is

$$\frac{\delta P}{P_0} = -3\gamma \frac{\delta R}{R_0} \quad (9.8)$$

Using this and the newton's second law for the equilibrium model, we get

$$\frac{d^2(\delta R)}{dt^2} = -(3\gamma - 4) \frac{GM}{R_0^3} \delta R \quad (9.9)$$

If  $\gamma > 4/3$ , the equation is that of simple harmonic motion where

$$\omega^2 = (3\gamma - 4) \frac{GM}{R_0^3} \quad (9.10)$$

with period

$$\Pi = \frac{2\pi}{\sqrt{\frac{4}{3}\pi G\rho_0(3\gamma - 4)}} \quad (9.11)$$

where  $\rho_0 = M/\frac{4}{3}\pi R_0^3$  is the average density of the equilibrium model.

If  $\gamma < 4/3$  we have a dynamically unstable model where  $\delta R = Ae^{-\kappa t}$ , which means that the increase in gas pressure is not enough to overcome the pull of gravity, resulting in a collapse.

## 9.4 Non-radial Stellar Pulsation

### 9.4.1 p-modes

For the case of non radial oscillations, the sound waves can propagate horizontally as well as vertically to produce waves that travel around the star. Because pressure provides the restoring force for these waves, the non radial oscillations are called p-modes. An estimate of the angular frequency of a p-mode may be obtained from the time for a sound wave to travel one horizontal wavelength, from one angular nodal line to the next. This horizontal wavelength is given by the expression

$$\lambda_h = \frac{2\pi r}{l(l+1)} \quad (9.12)$$

where  $r$  is the radial distance from the center of the star. The acoustic frequency at this depth is defined as

$$S_l = \frac{2\pi}{\text{time for sound to travel } \lambda_h}$$

Using the adiabatic sound speed, we finally get

$$S_l = \sqrt{\frac{\gamma P}{\rho}} \frac{\sqrt{l(l+1)}}{r} \quad (9.13)$$

### 9.4.2 g-modes and the buoyancy frequency

Gravity is the restoring force for another class of nonradial oscillations called g-modes. The waves involve a 'sloshing' back and forth of the stellar gases which is ultimately connected to the buoyancy of the stellar material.

Consider a bubble of stellar material that is displaced upward from its equilibrium position in the star by an amount  $dr$ . Assume that this motion occurs slowly enough that the pressure inside the bubble  $P^{(b)}$  is always equal to the pressure outside the bubble  $P^{(s)}$  and rapidly enough that there is no heat exchanged with the surroundings. Thus the net restoring force per unit volume on the bubble, through the Archimedes Principle is given by

$$f_{net} = (\rho_f^{(s)} - \rho_f^{(b)})g$$

where the  $f$  subscript denotes final values and  $g$  is the local acceleration due to gravity. Using a Taylor expansion for the densities about their initial positions results in

$$f_{net} = \left( \frac{d\rho^{(s)}}{dr} - \frac{d\rho^{(b)}}{dr} \right) g dr$$

Using the adiabatic relation between density and pressure for the bubble, and noting that initial densities of bubble and surroundings to be equal, we write

$$f_{net} = \left( \frac{1}{\rho} \frac{d\rho}{dr} - \frac{1}{\gamma P} \frac{dP}{dr} \right) \rho g dr \quad (9.14)$$

where we have dropped the superscripts and understood that all the quantities are of the stellar material outside the bubble. Taking the first term in the brackets as  $A$  we can say that if  $A > 0$ , the bubble continues to rise (which is nothing but the condition for stellar convection), and if  $A < 0$ , the bubble will oscillate about its equilibrium position simple harmonically. Thus for the second case, the acceleration is

$$a = -N^2 dr = Ag dr$$

where  $N$  is the angular frequency of the bubble about its equilibrium position, called the Brunt-Väisälä frequency or the buoyancy frequency,

$$N = \sqrt{-Ag} = \sqrt{\left( \frac{1}{\rho} \frac{d\rho}{dr} - \frac{1}{\gamma P} \frac{dP}{dr} \right) \rho g} \quad (9.15)$$

Inside convection zones, this frequency is not defined.

# Chapter 10

## Degenerate Remnants of Stars

### 10.1 White Dwarfs

White dwarfs are a class of stars that have approximately the mass of the Sun and size of the Earth. These stars occupy a narrow sliver in the HR diagram parallel to and below the main sequence. An estimate made of central conditions of pressure and temperature tell us that thermonuclear reactions are not involved in producing energy radiated by white dwarfs and that their centers consist of particles incapable of fusion. White Dwarfs are manufactured in the cores of low and intermediate mass stars.

#### 10.1.1 Physics of Degenerate Matter

We now answer the question what can support a white dwarf against the relentless pull of gravity if not thermonuclear reactions? The Pauli Exclusion principle allows at most one fermion in a quantum state because no two fermions can have the same quantum number. This means that even at 0 K, the fermions occupy the lowest excited states as the ground state is completely filled. The vigorous motion of the fermions in their excited states results in a *degeneracy* pressure, a pressure that exists not because of thermal motion but because of the Pauli Exclusion Principle.

From the Fermi-Dirac statistics it is possible to derive that the Fermi energy, the maximum energy of an electron in a completely degenerate gas at  $T = 0$  K, is given by

$$\epsilon_F = \frac{\hbar^2}{2m} (3\pi^2 n)^{2/3} \quad (10.1)$$

where  $n = N_e/L^3$  is the no. of electrons per unit volume and  $m$  is the mass of the electron. Assuming complete ionization, we can write  $n_e$  as

$$n_e = \left(\frac{Z}{A}\right) \frac{\rho}{m_H} \quad (10.2)$$

Thus we can write Fermi energy as

$$\epsilon_F = \frac{\hbar^2}{2m_e} \left(3\pi^2 \left(\frac{Z}{A}\right) \frac{\rho}{m_H}\right)^{2/3} \quad (10.3)$$

In rough terms, if the thermal energy is lesser than the Fermi energy, the electron will not be able to make a transition to an unoccupied state and the gas will remain degenerate. This can be taken as a condition for degeneracy.

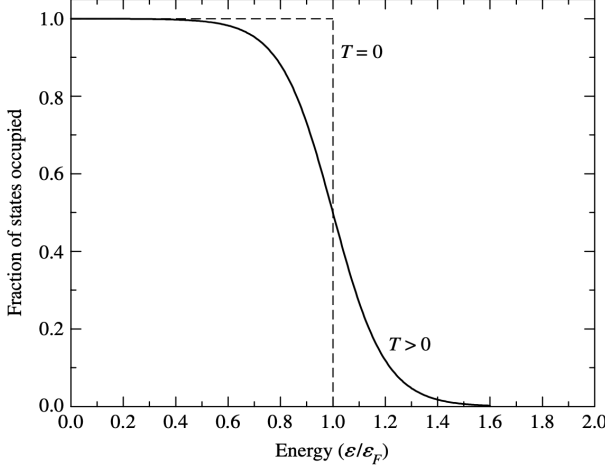


Figure 10.1: Fraction of states of energy  $\epsilon$  occupied by fermions [1].

$$\frac{3}{2}kT < \frac{\hbar^2}{2m_e} \left( 3\pi^2 \left( \frac{Z}{A} \right) \frac{\rho}{m_H} \right)^{2/3}$$

or

$$\frac{T}{\rho^{2/3}} < \frac{\hbar^2}{3m_e k} \left[ \frac{3\pi^2}{m_H} \left( \frac{Z}{A} \right) \right]^{2/3} = 1261 \text{ Km}^2 \text{kg}^{-2/3} \equiv D$$

for  $Z/A = 0.5$ . Thus the condition for degeneracy can be written as

$$\frac{T}{\rho^{2/3}} < D \quad (10.4)$$

### 10.1.2 Electron Degeneracy Pressure

We now combine the two key ideas of Quantum Mechanics; the Pauli Exclusion Principle and the Heisenberg Uncertainty Principle. From the pressure integral calculated in the Interior of Stars chapter, we can write

$$P \approx \frac{1}{3} n_e p v \quad (10.5)$$

assuming all electrons have the same momentum. Identifying  $\Delta x \approx n_e^{-1/3}$  for the limiting case of complete degeneracy, we use the uncertainty principle to estimate momentum. In one coordinate direction,

$$p_x \approx \Delta p_x \approx \frac{\hbar}{\Delta x} \approx \hbar n_e^{1/3}$$

In a 3D gas, each of the three directions are equally likely. Hence

$$p = \sqrt{3} p_x$$

Thus for full ionization,

$$p \approx \sqrt{3} \hbar \left[ \left( \frac{Z}{A} \right) \frac{\rho}{m_H} \right]^{1/3} \quad (10.6)$$

For non-relativistic electrons the speed is  $v = p/m_e$ . Using this in eq. 10.5, we have the degeneracy pressure to be

$$P \approx \frac{\hbar^2}{m_e} \left[ \left( \frac{Z}{A} \right) \frac{\rho}{m_H} \right]^{5/3} \quad (10.7)$$

A more exact treatment gives the degeneracy pressure of a completely degenerate, nonrelativistic electron gas  $P$  to be

$$P = \frac{(3\pi^2)^{2/3}}{5} \frac{\hbar^2}{m_e} \left[ \left( \frac{Z}{A} \right) \frac{\rho}{m_H} \right]^{5/3} \quad (10.8)$$

Using  $Z/A = 0.5$  we get a pressure within a factor or two of our previous estimate of the central pressure of a white dwarf. Thus *electron degeneracy pressure is responsible for maintaining hydrostatic equilibrium in a white dwarf.*

### 10.1.3 Chandrashekhar Limit

The estimate of the central pressure can be made by taking the white dwarf to be of constant density and using this to integrate the first stellar structure equation. Setting this pressure equal to the degeneracy pressure and solving for the radius, we have

$$R_{wd} \approx \frac{(18\pi^2)^{2/3}}{10} \frac{\hbar^2}{Gm_e M_{wd}^{1/3}} \left[ \left( \frac{Z}{A} \right) \frac{\rho}{m_H} \right]^{5/3} \quad (10.9)$$

This leads to the surprising implication that

$$M_{wd} V_{wd} = \text{constant} \quad (10.10)$$

The more massive the white dwarf, the smaller its radius is. With this, an upper limit to the mass of the white dwarf can be estimated because there exists a limit to the speed of electrons in the white dwarf responsible for maintaining the degeneracy pressure. This limit is nothing but the speed of light.

In the extreme relativistic limit we use  $v = c$  to calculate the electron degeneracy pressure from eq. 10.5 to be

$$P = \frac{(3\pi^2)^{1/3}}{4} \hbar c \left[ \left( \frac{Z}{A} \right) \frac{\rho}{m_H} \right]^{4/3} \quad (10.11)$$

The smallest departure from this equilibrium value will result in the collapse of the white dwarf as electron degeneracy pressure fails. An approximate value of the maximum mass of the white dwarf can be obtained by setting this pressure equal to the central pressure estimate. The radius cancels off to give

$$M_{Ch} \sim 0.44 M_\odot \quad (10.12)$$

A precise treatment actually leaves us with a value of  $M_{Ch} = 1.44 M_\odot$ .

### 10.1.4 Cooling of White Dwarfs

In a white dwarf, energy is carried by electron conduction rather than by radiation. This is so efficient that the interior of a white dwarf is nearly isothermal, with the temperature dropping significantly only in the nondegenerate surface layers. It can be derived from the degeneracy condition that the luminosity of the white dwarf is proportional to the interior temperature in the form

$$L_{wd} = CT_c^{7/2} \quad (10.13)$$

But the luminosity is also given by the Stefan's law. Studying the two relations surprisingly reveals that the surface of the white dwarf cools more slowly than the interior.

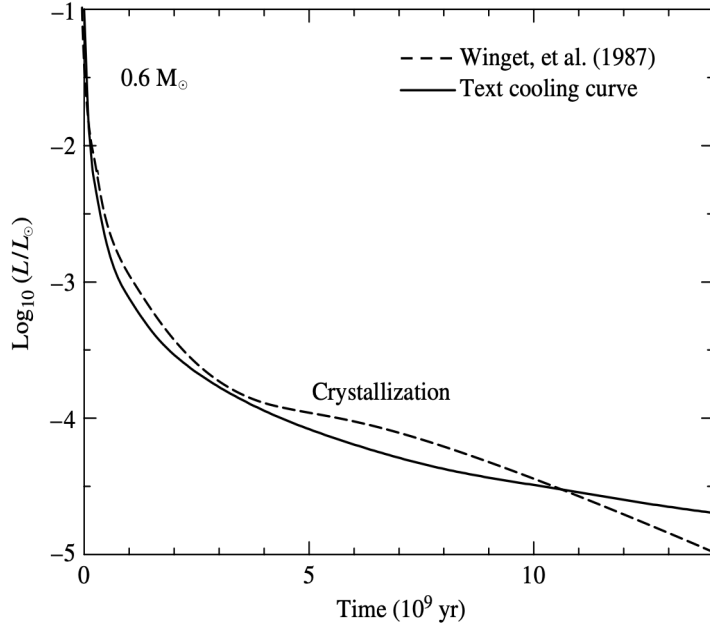


Figure 10.2: Theoretical and observed cooling curves for a  $0.6M_{\odot}$  white dwarf [1].

An estimate of the total thermal energy available for radiation is

$$U \approx \frac{M_{wd}}{Am_H} \frac{3}{2} k T_c$$

A crude estimate of the characteristic timescale for cooling is

$$\tau_{cool} = \frac{U}{L_{wd}} \quad (10.14)$$

To obtain temperature as a function of time we solve the differential equation

$$-\frac{dU}{dt} = L_{wd}$$

Substituting the necessary terms and integrating, we get

$$T_c(t) = T_0 \left(1 + \frac{t}{\tau_0}\right)^{-2/5} \quad (10.15)$$

where  $\tau_0 = \tau_{cool}$  and  $T_0$  is the initial internal temperature at  $t = 0$ . Using eq. 10.13, we also have luminosity as a function of time and when plotted, it is in close agreement with observational data (Fig. 10.2).

A slight discrepancy occurs between the two plots (theoretical and observed), as the observed luminosity slightly exceeds the theoretical luminosity for some time. This can be explained by considering the phenomenon of crystallization, wherein the nuclei of the white dwarf undergo a phase change and crystallize, releasing their latent heat and slowing the cooling process. After this point the crystallized lattice accelerates the cooling process. Thus the ultimate monument to the lives of most stars will be a "diamond in the sky", a cold, dark, earth-size sphere of crystallized carbon and oxygen floating through the depths of space.

## 10.2 Neutron Stars

### 10.2.1 Formation and Properties

As massive stars evolve off the main sequence carbon, oxygen and silicon burning produces lesser and lesser energy as the products near the iron peak in the binding energy curve. Thus the pressure supporting the overlying layers decreases resulting in a collapse. Density increases so much that the free electrons that had assisted in supporting the star through degeneracy pressure are captured by heavy nuclei and by the protons.

$$p^+ + e^- \rightarrow n + \nu_e \quad (10.16)$$

The amount of energy that escapes the star in the form of neutrinos becomes enormous and a series of shock waves resulting from rebounds of the infalling material with the dense neutron-rich core ultimately results in a core-collapse supernova leaving behind a neutron star.

Transition density (kg m <sup>-3</sup> )	Composition	Degeneracy pressure
$\approx 1 \times 10^9$	iron nuclei, nonrelativistic free electrons	electron
	electrons become relativistic	
$\approx 1 \times 10^{12}$	iron nuclei, relativistic free electrons	electron
	neutronization	
$\approx 4 \times 10^{14}$	neutron-rich nuclei, relativistic free electrons	electron
	neutron drip	
$\approx 4 \times 10^{15}$	neutron-rich nuclei, free neutrons, relativistic free electrons	electron
	neutron degeneracy pressure dominates	
$\approx 2 \times 10^{17}$	neutron-rich nuclei, superfluid free neutrons, relativistic free electrons	neutron
	nuclei dissolve	
$\approx 4 \times 10^{17}$	superfluid free neutrons, superconducting free protons, relativistic free electrons	neutron
	pion production	
	superfluid free neutrons, superconducting free protons, relativistic free electrons, other elementary particles (pions, ...?)	neutron

Figure 10.3: A summary of the composition of neutron star material at various densities [1].

Neutron stars are in effect huge nuclei of mass number  $A = 10^{57}$  held together by gravity and supported by neutron degeneracy pressure. Similar to white dwarfs, the radius of neutron stars can be derived to be

$$R_{ns} \approx \frac{(18\pi^2)^{2/3}}{10} \frac{\hbar^2}{GM_{ns}^{1/3}} \left( \frac{1}{m_H} \right)^{8/3} \quad (10.17)$$

An estimate of the average density of a neutron star gives us  $\rho \approx 6.65 \times 10^{17} \text{ kg/m}^3$ , which is much greater than the density of atomic nuclei.

Like white dwarfs, neutron stars obey the relation

$$M_{ns}V_{ns} = \text{constant} \quad (10.18)$$

Analogous to the Chandrasekhar limit for white dwarfs, the maximum mass of a nonrotating neutron star that can be supported by neutron degeneracy pressure can be derived to be  $2.2M_\odot$ , and for rapidly rotating neutron stars (pulsars) to be  $2.9M_\odot$ . If the mass exceeds these values, the star collapses to form a black hole.

### 10.2.2 Rapid Rotation and Conservation of Angular Momentum

It was theorized that neutron stars must be rotating very rapidly due to the conservation of angular momentum. If we assume the progenitor core of the neutron star to be a white dwarf composed entirely of iron, we arrive at the ratio of radii, using the equations of radii of white dwarfs and neutron stars, to be

$$\frac{R_{core}}{R_{ns}} \approx \frac{m_n}{m_e} \left( \frac{Z}{A} \right)^{5/3} = 512 \quad (10.19)$$

Assuming no mass loss, from the conservation of angular momentum we have

$$\omega_f = \omega_i \left( \frac{R_i}{R_f} \right)^2$$

Thus the rotation period of the neutron star is

$$P_{ns} = 3.8 \times 10^{-6} P_{core} \quad (10.20)$$

Estimates give us the rotation period to be of the order of a few milliseconds.

### 10.2.3 Magnetic Fields

Another property predicted for neutron stars was very high magnetic fields. An estimate of the neutron stars magnetic field in terms of the progenitor white dwarf core's magnetic field can be made using the conservation of magnetic flux. This is because of the "freezing-in" of magnetic field lines in conducting fluids and gases. Thus roughly,

$$B_i 4\pi r_i^2 = B_f 4\pi r_f^2 \quad (10.21)$$

Taking the magnetic field of a pre-supernova core to be around  $B \approx 5 \times 10^4 \text{ T}$ , we have

$$B_{ns} \approx B_{wd} \left( \frac{R_{wd}}{R_{ns}} \right)^2 = 1.3 \times 10^{10} \text{ T} \quad (10.22)$$

This shows that neutron stars have very high magnetic fields although values of  $10^8 \text{ T}$  are more typical.

# Bibliography

- [1] Bradley W. Carroll, Dale A. Ostlie. *An Introduction to Modern Astrophysics*. Pearson, 2014.
- [2] Hans A. Bethe, Gerald Brown. *How a Supernova Explodes*. Physics, 1985
- [3] *Sloan Digital Sky Survey/ Sky Server* <http://cas.sdss.org/dr7/en/proj/advanced/spectra/types/lines.asp>